REVIEW

Check for updates

Enhanced biochemical sensing using metallic nanoclusters integrated with metal–organic frameworks (NCs@MOFs): a comprehensive review

Sameera Sh. Mohammed Ameen, [iD] *[a] Khalid M. Omer, [iD] *[b] Farzaneh Shalileh[c] and Morteza Hosseini*[c]

In biochemical sensing, substantial progress has been achieved in the design, development, and application of metallic nanoclusters (NCs) and metal–organic frameworks (MOFs) as distinct entities. Integration of these two nanostructured materials is a promising strategy to form innovative composites with improved properties. Some improvements include (i) supporting platform to minimize the aggregation of NCs and enhance the emission efficiency; (ii) dual-emitting NCs@MOFs from the fluorescent/ non-fluorescent MOFs and/or fluorescent NCs; and (iii) stability enhancement. These improvements increase the sensitivity, signal-to-noise ratio, and color tonality, lower the limit of detection, and improve other analytical figures of merits. In this review, we outline the preparation methods of NCs@MOF composites with the improvements offered by them in the field of biochemical analysis. Analytical applications in different fields, such as bioanalysis, environmental monitoring and food safety, are presented. Finally, we address the challenges that remain in the development and application of these composites, such as ensuring stability, enhancing the fluorescence intensity, and improving selectivity and scalability. Furthermore, perspectives on future research directions in this rapidly evolving field are offered.

Wider impact

This review highlights the transformative potential of NCs@MOF composites in biochemical sensing, offering enhanced sensitivity, stability, and detection efficiency for diverse applications in bioanalysis, environmental monitoring, and food safety. By addressing challenges like scalability, selectivity, and fluorescence intensity, these composites pave the way for more precise diagnostics, pollutant detection, and food safety monitoring. The insights provided here aim to inspire innovation and guide the scientific community toward developing next-generation sensing platforms that bridge the gap between research and real-world applications.

1. Introduction

Sensing technologies play a pivotal role in various areas, including healthcare, manufacturing, environmental monitoring, and agriculture, by enabling the real-time detection, measurement, and analysis of physical, chemical, and biological phenomena. Integration of nanotechnology and advanced nanomaterials has significantly enhanced the performance of

sensing devices. The use of nanotechnology also enables the miniaturization of sensors, making them portable and suitable for use in challenging environments.[1–4] A variety of nano-materials have been developed in recent years. Nanomaterials such as metallic nanoclusters (NCs) and metal–organic frameworks (MOFs) offer higher sensitivity, greater selectivity, and improved stability, allowing for the development of more accurate and reliable sensors.

Recently, there has been a rapid progress in the development of atomically precise metal nanoclusters (NCs), including advancements in their synthesis methods and potential applications.[5,6] NCs are particularly significant in sensing and catalysis owing to their unique geometric and electronic characteristics.[7] They exhibit the highest degree of uniformity, precise atomic compositions, and clearly defined atomic

[a] Department of Chemistry, College of Science, University of Zakho, Zakho, Kurdistan region, 42002, Iraq. E-mail: sameera.m.ameen@uoz.edu.krd

[b] Department of Chemistry, College of Science, University of Sulaimani, Qliasan St. 46002, Sulaymaniyah, Kurdistan region, Iraq. E-mail: khalid.omer@univsul.edu.iq

[c] Nanobiosensors Lab, Department of Life Science Engineering, Faculty of New Sciences & Technologies, University of Tehran, Tehran, Iran. E-mail: hosseini_m@ut.ac.ir

packing arrangements, which facilitate the exploration of structure–reactivity relationships. For example, gold nanoclusters (AuNCs) are used for the detection of tumors and other diseases as they can be designed to target specific cells or tissues. Additionally, copper nanoclusters (CuNCs) are used in both *in vitro* and *in vivo* theranostic applications, enabling the detection and treatment of diseases.[8–11]

However, there are two key challenges in using NCs: (1) their insufficient stability under harsh conditions, such as a tendency to aggregate, and (2) the steric hindrance caused by ligands, which can impede bulky reactants.[12] The high surface free energy associated with their ultrafine size contributes to a high tendency for the NCs to aggregate, especially at elevated temperatures, leading to a significant reduction in active sites.[13] Thus, enhancing the catalytic performance involves stabilizing NC structures while mitigating the shielding effect of ligands on the metal sites.

To address the above-mentioned problems, one of the effective strategies is to integrate NCs with other porous and high surface area platforms, such as metal–organic frameworks (MOFs). MOFs have emerged as a promising class of materials for biochemical sensing owing to their unique properties, such as high surface area, tunable pore size, and chemical stability.[14–21] MOFs can be designed to selectively bind to specific biomolecules, such as proteins, nucleic acids, or small molecules, allowing for the development of highly sensitive and selective biosensors. For instance, MOFs can be functionalized with specific ligands to recognize and bind to target biomolecules, which can then be detected through changes in fluorescence, absorbance, or other optical properties.[22–27] This enables the detection of biomarkers for various diseases, such as cancer, diabetes, or neurological disorders, with high accuracy and sensitivity. Additionally, MOFs can be integrated with other sensing technologies, such as electrochemical or piezoelectric sensors, to enhance their detection capabilities.[28] Overall, MOFs offer a powerful platform for the development of next-generation biochemical sensors with high sensitivity, selectivity, and versatility.[29–31]

The synergy between combining two materials, such as MOFs and NCs, has been not been well-explored in biochemical sensing applications. The porous structure of MOFs and their adjustable pore sizes make them ideal hosts for precisely integrating nanoclusters, allowing control over their size, composition, and dispersion within the matrix.[32] Moreover, the tailored binding sites within MOFs can selectively target specific analytes, improving the sensor's ability to distinguish desired compounds, while reducing interference from background substances. Additionally, the confinement effect within MOFs enhances the stability and lifespan of nanoclusters, ensuring sustained sensor performance. This synergy can lead to enhanced sensing performance, improved stability, selectivity, and increased sensitivity.

The aim of this review is to provide a comprehensive analysis of the latest developments in atomically precise NCs, and their incorporation with MOFs for applications in biochemical sensing. This review will focus on the critical challenges associated with the stability and functionality of NCs, offering insights into how these obstacles can be addressed. Additionally, it will highlight the synergistic advantages gained

from combining NCs with MOFs, which significantly enhance the sensitivity, selectivity, and durability of the sensors. By exploring these advancements, the review aims to outline the potential of MOF-NC composites in revolutionizing the field of biosensing and fostering the development of highly advanced, next-generation biosensors. Our review stands out as the first comprehensive analysis focusing specifically on the integration of atomically precise NCs with MOFs for biochemical sensing applications. While previous reviews have addressed NCs or MOFs independently in various sensing domains, none have explored the synergistic interplay between these two advanced materials in such depth. This review not only highlights the critical challenges associated with the stability and functionality of NCs but also provides unique insights into how their incorporation into MOFs can address these limitations, enhancing the sensor performance in terms of sensitivity, selectivity, and durability.
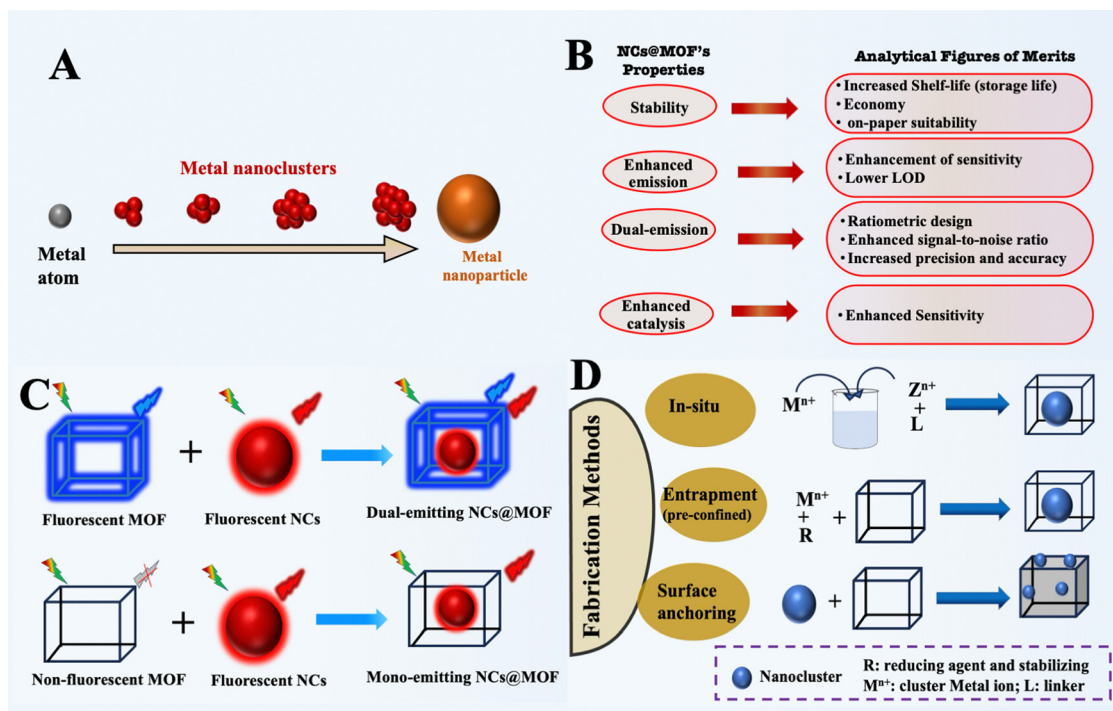
2. An overview of metallic nanoclusters (NCs) and metal organic frameworks (MOFs), and their integration

As mentioned earlier, NCs and MOFs are two types of nanomaterials that have gained much attention for the advancement of sensing technologies in recent years. In this section, a comprehensive overview of these nanostructures and their integrated form is provided.

2.1. Metallic nanoclusters (NCs)

Metallic nanoclusters (NCs) are ultra-small clusters of metal atoms, typically less than 2 nanometers in size, with unique properties due to quantum confinement effects.[32,33] These clusters exhibit distinct optical and catalytic behaviors that differ from those of bulk metals or larger nanoparticles (nano-scale materials bigger than 3 nm), as shown in Scheme 1A. Their exceptional sensitivity to environmental changes, combined with tunable characteristics through precise control over size, composition, and surface chemistry, makes them particularly valuable in various applications, including catalysis and sensing.[34,35] These NCs are frequently stabilized by ligands or other molecules that inhibit aggregation and help preserve their unique properties.

In biochemical sensing, metallic NCs offer enhanced sensitivity and specificity, allowing for the detection of minute concentrations of biomolecules with high precision. Their surfaces can be functionalized to target specific analytes, improving selectivity. Additionally, their ability to emit at distinct wavelengths or respond to various analytes enables multiplexing, making them versatile tools in diagnostics, environmental monitoring, and biomedical research.[36,37] Their biocompatibility further extends their potential use in *in vivo* sensing applications, providing a powerful platform for real-time detection and the monitoring of biological processes.

Scheme 1 (A) Comparison of the sizes between an atom, a nanocluster and nanoparticles. (B) Improved analytical figures of merits of NCs@MOFs. (C) Fluorescent and/or non-fluorescent MOFs with NCs. (D) Different fabrication methods of NCs@MOF nanocomposites.

NCs face specific challenges that must be addressed to expand their applications. A primary concern is their instability, which often leads to aggregation and a loss of their distinctive properties. This instability arises from their high surface free energy, a consequence of their extremely small size. To address this problem, encapsulation within the framework is one strategy that can be used to increase the NCs' stability, such as using MOF. From here, synergism of the properties of both NCs and MOFs arises and new phenomena also evolve, such as dual-emitting fluorescence (Scheme 1B).

2.2. Metal–organic frameworks (MOFs)

Metal–organic frameworks (MOFs) are crystalline materials formed by metal ions or clusters linked by organic ligands, creating a highly structured network.[38–44] These frameworks are characterized by their large surface areas, high porosity, and adjustable pore sizes.[45–48] Their chemical versatility and unique structural properties make MOFs suitable for diverse applications, including gas storage, catalysis, and drug delivery.[49–52]

MOF synthesis usually occurs through solvothermal or hydrothermal methods, where metal salts react with organic ligands in a solvent under high temperatures. By altering the metal ions, organic ligands, and reaction conditions like temperature, pressure, and solvent, the properties of the MOF can be tailored.[53–55] Due to their unique structures, MOFs are highly adaptable to integration with other functional nanomaterials, and can act as precursors or templates to prepare MOF-based composites with exceptional physical and chemical characteristics.[56,57]

MOFs have several characteristics that make them highly suitable for chemical sensing, such as their high porosity and extensive surface area, which facilitate strong interactions with target molecules, boosting detection sensitivity. MOFs' customizable pore sizes and selective structures enhance their ability to capture specific analytes, improving selectivity even in complex samples.[58] Additionally, MOFs can be functionalized with specific binding sites or reactive groups to target particular chemicals. Some MOFs also exhibit luminescent properties, which can be used in fluorescence-based detection, enabling sensitive optical signals.[22,59] Together, these properties make MOFs versatile and reliable platforms for chemical sensing in diverse applications.[50,51,60–63]

Despite their promising characteristics, MOFs still face several limitations in practical applications for sensing. While MOFs offer high porosity, customizable structures, and chemical functionality, they often exhibit limited selectivity, especially when used in complex matrices with multiple analytes. This low selectivity can result in interference from other substances, reducing the accuracy of the detection process. Additionally, multiplex analysis in complicated matrices remains challenging, as MOFs may struggle to differentiate between structurally similar molecules. MOFs also face issues with stability; some frameworks degrade under harsh environmental conditions, which limits their long-term usability and reliability. Lastly, the sensitivity of MOFs in detecting low-concentration analytes can sometimes be insufficient, particularly when compared to other advanced sensing materials. Addressing these limitations is crucial for advancing the utility of MOFs in real-world sensing applications.

MOFs have been integrated with other nanomaterial entities to enhance their functionalities and capacities, such as with molecular imprinted polymers (MIPs),[64] metal oxides,[65] metal nanoparticles,[66] antibodies,[67] and carbon dots.[68]

NCs are another alternative promising material that can be used to form a hybrid composite *via* merging with MOFs. This integration helps to overcome the individual limitations of each material, and produces distinctive new properties (Scheme 1B). All the improved characteristics affect the figures of merits in biochemical-based probes for sensing applications.

2.3. NCs @MOFs nanocomposites with fabrication methods

One of the promising strategies to mitigate the limitations of NCs and MOFs is their integration as NCs@MOFs. This section comprehensively discusses the methods for their integration and the associated advantages.

A variety of methods can be leveraged for the synthesis of NCs@MOF nanocomposites, which are introduced below.

2.3.1. Surface anchoring. Surface anchoring is the simplest approach for integrating or immobilizing NCs with MOFs, often achieved through a basic wet impregnation process. Generally, combining pre-synthesized MOFs and NCs in a single step can attach the NCs to the MOF's outer surface, provided that the NCs are larger than the pore size of the MOF matrices.[69]

2.3.2. *In situ* method. *In situ* synthesis is a method for the preparation of materials or compounds directly within its original reaction medium, rather than first synthesizing them separately and then incorporating it into the final system. In materials science, this approach means forming the compound or material at the site where it will be applied, which can improve integration and enable more precise or efficient production. Here, *in situ* synthesis involves the preparation of nanoclusters and MOF during the formation of both, rather than adding pre-made nanoparticles afterward.

Li *et al.*[70] have *in situ* prepared CuNCs using Cu-MOF as the template and 2,3,5,6-tetrafluorobenzenethiol (TFTP) as the redundant, as shown in Fig. 1A.

2.3.3. Entrapment method (pre-confined). In this method, the prepared nanoclusters are introduced into the MOF structure. This can be achieved by adding the nanocluster solution to the MOF precursor solution or by post-synthetic methods, where the nanoclusters are introduced into pre-formed MOF structures.[71]

CuNCs@ZIF-8 were prepared after the synthesis of nanoclusters, followed by mixing with ZIF-8 precursors.[71] As shown in Fig. 1B, Zn^{2+} ions and CuNCs are combined, and then 2-methyl imidazole (2 Mlm) is added to form ZIF-8, while simultaneously incorporating CuNCs. The process of incorporating CuNCs into ZIF-8 might occur in two stages. In the initial stage, a coordination complex forms between Zn^{2+} and CuNCs, resulting in the neutralization of the surface charge of CuNCs, as evidenced by the change in the zeta potential of the particles from negative to positive. In the second stage, Zn^{2+} ions detach from the surface of CuNCs, leading to the formation of CuNC/ZIF-8 composites, driven by the strong binding affinity of 2-MIm for Zn^{2+} ions.
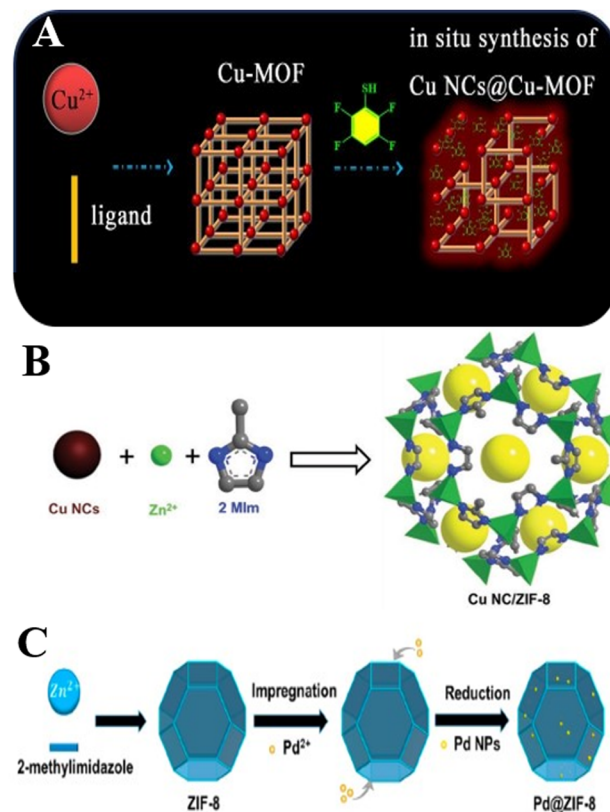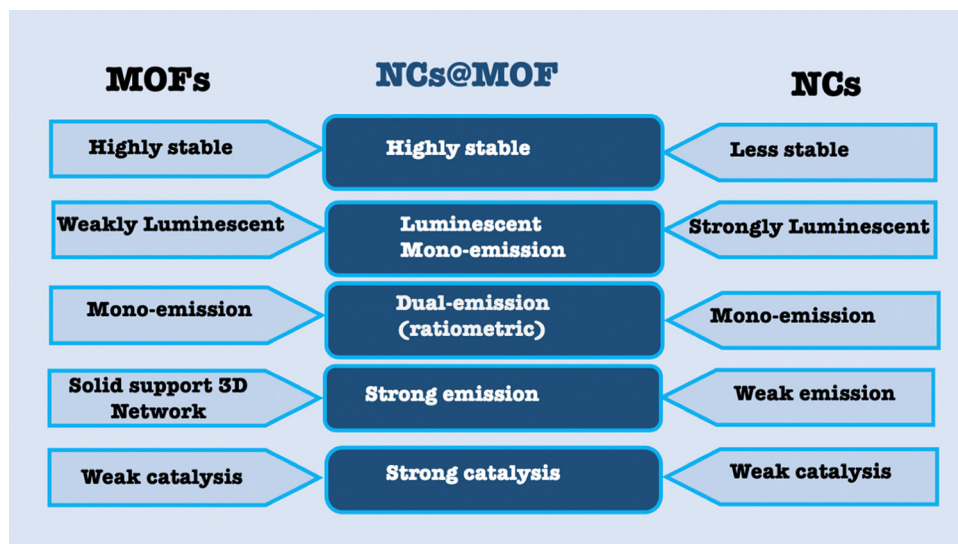

Fig. 1 (A) Diagram of the synthesized probe. Reproduced with permission from Elsevier.[70] (B) Preparation of a nanocomposite of CuNCs@ZIF-8 *via* an entrapment method. Reproduced with permission from Wiley.[71] (C) Representative scheme of the synthesis of Pd@ZIF-8. Reproduced with permission from the American Chemical Society.[72]

Li *et al.*[72] used the entrapments (impregnation) method to prepare Pd NCs inside the ZIF-8 (Fig. 1C). In this work, PdNCs with an average size of 1.4 nm were synthesized using ZIF-8 as a matrix *via* an impregnation-reaction (entrapment) method. The advantage of this method is the ability to obtain small size PdNPs within the confined channels of ZIF-8. Furthermore, due to the strong chemical interaction between PdNCs and ZIF-8, the clusters are highly stable.

3. Improved characteristics of NCs@MOF nanocomposites

As previously noted, metallic NCs face several significant challenges, including low fluorescence quantum yield, limited catalytic activity, and inherent instability. These limitations restrict their broader application in various fields. On the other hand, MOFs offer a range of valuable properties, such as high porosity, large surface area, and a tunable surface structure, along with customizable luminescence. By combining these two nanostructures, NCs and MOFs, the strengths of each can be harnessed to counterbalance the weaknesses of the other (Scheme 2). This integration results in the formation of hybrid materials that exhibit unique and enhanced properties, such as

Scheme 2 A scheme summarizing the enhanced properties of NCs@MOFs.

improved stability, higher fluorescence yield, and increased catalytic performance. This synergy opens up new possibilities for advanced applications in sensing, catalysis, and beyond.

3.1. Stability

The stability of nanomaterials in sensors is crucial for ensuring the accurate and reliable detection over time, especially when exposed to varying environmental conditions, such as temperature fluctuations, humidity, storage time, or chemical interactions.[73] Stability refers to the material's ability to maintain its physical, chemical, and functional properties under these conditions, which is essential for preventing degradation, structural changes, or loss of performance. Unstable materials can lead to inaccurate readings, reduced sensitivity, and sensor degradation, compromising the entire sensing process. For a sensor to be effective in real-world applications like medical diagnostics, environmental monitoring, or industrial applications, the material must resist factors such as extreme temperatures, moisture, and prolonged chemical exposure. Achieving long-term stability enhances the sensor's durability, lifespan, and ensures high sensitivity, selectivity, and reproducibility, all of which are critical for the reliable and consistent detection of target analytes.

NCs@MOF nanocomposites increases the stability of nanoclusters due to the decreased aggregation of the clusters or decreased metal oxidation inside the MOF.[71] In CuNCs@ZIF-8, the fluorescence intensity of pure CuNCs is rapidly quenched under ambient conditions, with a reduction of over 50% in 5 hours. In contrast, CuNC@ZIF-8 showed only a minor decrease (less than 15%) in fluorescence intensity even after two weeks of storage. This enhanced stability is attributed to the protective effect of ZIF-8, which reduces the likelihood of oxidation of the metal core in the clusters.[71] Therefore, NCs@MOFs increases the shelf-life of the composite, improving its economic value by eliminating the need for daily or weekly preparation. This increased stability makes the composite highly suitable for off-site paper tests.

3.2. Enhanced luminescence

Enhanced luminescence is crucial for improving the sensitivity and accuracy of biochemical sensing, allowing for the detection of low concentrations of analytes. It enhances the signal-to-noise ratio, making it possible to identify subtle changes in analyte levels. This leads to the more precise detection of trace amounts of biological markers or pollutants, expanding the range and effectiveness of biochemical sensors.

Jalili et al.[74] prepared AuNCs@ZIF-8 and noticed significant enhancement of the fluorescence quantum yield by 15 times. They attributed this enhancement to the confinement-assisted emission enhancement. The confinement-assisted emission enhancement is the process where the luminescence of a material is amplified due to its physical or chemical confinement within a host structure, such as a porous framework or matrix. This enhancement occurs through various mechanisms, including the suppression of non-radiative decay by restricting molecular vibrations and motions, the rigidity of the host material minimizing energy dissipation, and the prevention of aggregation-induced quenching by spatially separating luminescent species.

Meanwhile, Xia et al.[75] prepared AuNCs@ZIF-8 and showed almost 7.0 times enhancement in the quantum yield, and longer fluorescence lifetime from 2.29 μs to 11.51 μs compared with AuNCs. This enhancement is due to aggregation-induced emission owing to the confinement effect.

3.3. Dual-emission design

Dual emission design is highly important for ratiometric and color tonality analysis.[76–79] In this context, NCs@MOFs can achieve dual-emission in many ways, as shown in Scheme 1C. The first approach uses one emitting NC with one emitting MOF.[80] The second approach involves a single emitting NC paired with an emitting fluorophore encapsulated within a non-emitting MOF. Here, we refer to a scenario with two distinct emitting fluorophores within the non-emitting MOF:

the first being NCs and the second potentially being a non-NC, such as an organic dye.[81] Ratiometric analysis utilizes dual-emission to measure the ratio of two different emission signals, which enhances the accuracy and reliability of detection. This technique improves the measurement precision by correcting for variations in the concentration, environmental conditions, or instrument performance. By evaluating the ratio of the two signals, ratiometric analysis ensures more consistent and sensitive detection of analytes, making it ideal for complex applications such as quantitative assays, environmental monitoring, and biomedical diagnostics. This method minimizes errors and helps distinguish between closely related substances.

Ma *et al.*[82] designed a ratiometric platform from blue fluorescent MOF, UiO-66-NH$_2$, with orange CuNCs. The ratiometric platform was used for the detection of glutathione.

4. Applications of NCs@MOFs in sensing applications

Metal NCs are integrated with different kinds of MOFs for various sensing applications. Herein, various NCs@MOFs that have been classified based on the types of metal nanoclusters and their applications in the sensing of various analytes in the

field of biochemistry are discussed. Table 1 provides a summary of various NCs@MOFs in biochemical sensing applications.

4.1 Au NCs@MOFs

AuNCs are gaining significant interest across various fields of nanotechnology. These tiny, sub-nanometer particles exhibit molecular-like electronic transitions between their HOMO and LUMO energy levels, as a consequence of their very small (finite) cluster size. Due to this distinctive electronic structure, Au NCs display notable photoluminescent properties, opening up exciting possibilities for optical applications.

Su *et al.*[107] have prepared 2D nanosheets of Zr-based MOF (521-MOF) embedded with AuNCs for the electrochemical aptasensor detection of cocaine (Fig. 2A). The AuNCs@Zr-MOFs were prepared under mild conditions *via* one-pot synthesis. The 2D AuNCs@Zr-MOF nanosheets showed a high specific surface area, physicochemical stability, good electrochemical activity, and strong affinity toward biomolecule-bearing phosphate groups. The cocaine aptamer strands can be attached to 2D AuNCs@Zr-MOF nanosheets, developing a selective and sensitive platform for cocaine. The cocaine aptamer was successfully immobilized onto the nanocomposite-modified electrode surface *via* robust π–π stacking interactions

Table 1   NCs@-MOFs in various fluorescence-based sensing applications

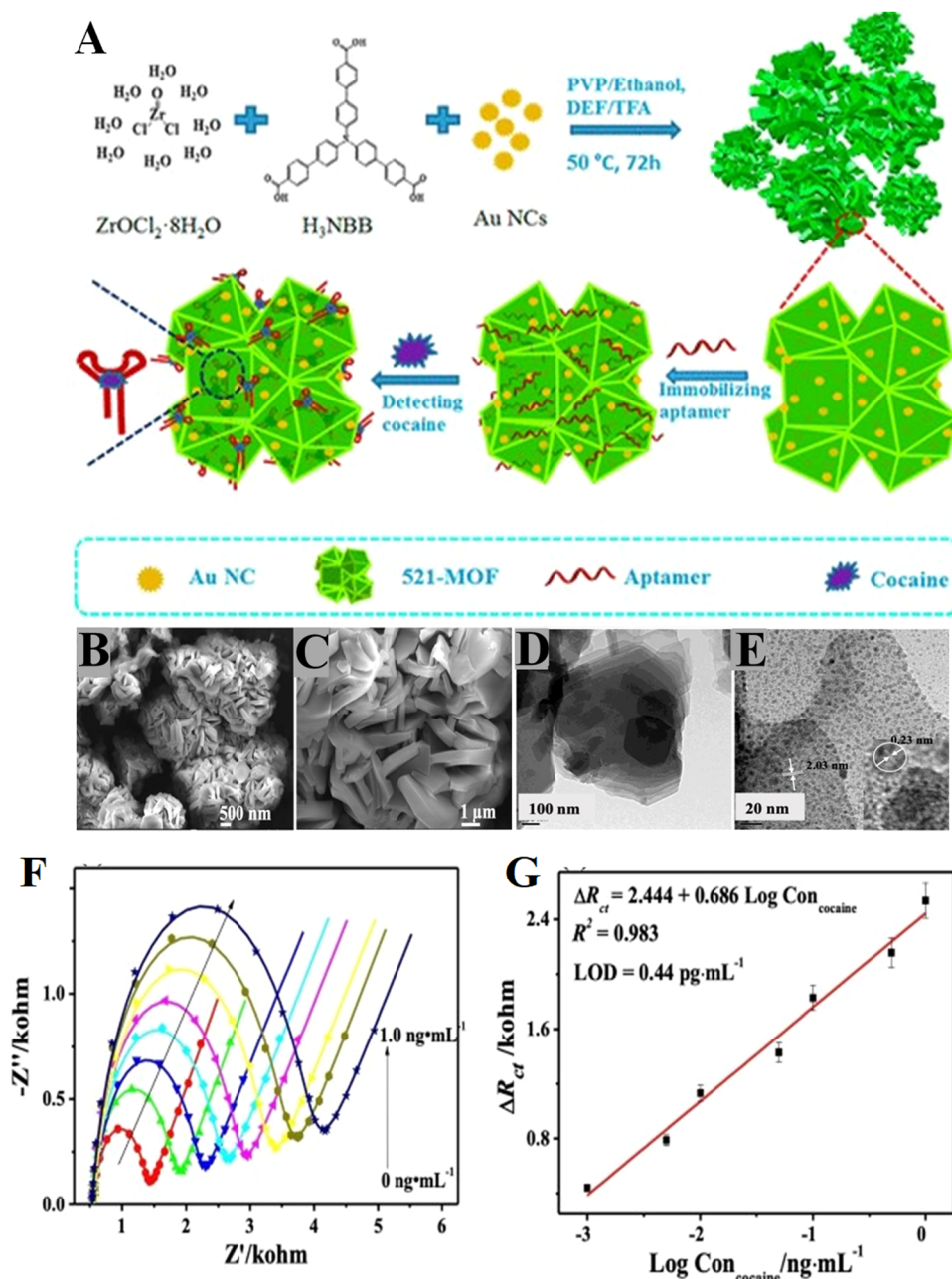| NCs@MOFs	Nanoclusters	Detection targets	Linearity range	LOD	Ref.
CD@ZIF-CuNC	CuNCs	Uric acid, H$_2$O$_2$	1–100 μM, 1–30 μM	0.30 μM, 0.33 μM	83
Cu NCs@Cu-MOF	CuNCs	H$_2$O$_2$	—	72.5 nM	70
		2,4-DNP	—	67 nM	
CuNCs/ZIF-8	CuNCs	H$_2$O$_2$	0.01–1.5 μM	0.01 μM	84
CuNCs@ZIF-8	CuNCs	Tetracycline	1.0–10.0 μM	0.30 μM	35
CNCs@ZIF-8	CNCs	Nitrofurazone, lysine	—	0.0229 μM	85
			—	0.0096 μM	
B-CuNCs@ MIP@ZIF-8	B-CuNCs	Ascorbic acid	4.0–22.0 μM	1.56 μM.	34
UiO-66-NH$_2$@Cu NCs	CuNCs	GSH, Cys	—	—	82
MOF@ CuNCs	CuNCs	Trinitrotoluene	—	—	86
Cu NCs@Tb-GMP	CuNCs	Alkaline phosphatase	0.002–2 U mL^{-1}	0.002 U mL^{-1}	87
CuNCs-Al^{3+}/ZIF-90	CuNCs	Adenosine triphosphate	1–2000 μM	0.67 μM	88
Cu NCs–Al@ZIF-90	CuNCs	Adenosine triphosphate	0.2–0.625 mM	0.034 mM	89
CuNCs@Tb@UiO-66-(COOH)$_2$	CuNCs	Cu^{2+}	—	—	90
CuNCs@ZrMOF	CuNCs	Al^{3+}	0–60 μM	139 nM	91
KA-Cu NC/MIL-53(Fe)	CuNCs	S^{2-}	0.05–5 μM	18 nM	92
AuCuNCs@MOF	AuNC and CuNC	Tetracycline	20–650 nM	4.8 nM	93
gCDc/AuNCs @ ZIF-8	AuNCs	Cephalexin	0.1–6 ng mL^{-1}	0.04 ng mL^{-1}	94
AuNCs@ZIF-8	AuNCs	3-Nitrotyrosine	5–200 nM	1.8 nM	74
AuNCs@ZIF-8	AuNCs	MicroRNA	—	—	95
CDs/AuNCs@ ZIF-8	AuNCs	Adenosine triphosphate	—	0.061 μM	96
AuNCs@ MOF	AuNCs	Adenosine triphosphate	—	—	97
AuNCs@ZIF-8	AuNCs	Acetylcholinesterase	—	0.4 mU mL^{-1}	81
GSH-Au NCs@ZIF-8	AuNCs	Rutin	—	10 nM	98
AuNCs@ZnGlu-MOFs	AuNCs	H$_2$O$_2$	—	—	99
CDs/AuNCs@ZIF-8	AuNCs	Cu^{2+}	10^{-3}–10^3 μM	0.3324 nM	100
GSH-Au NCs@ZIF-8	AuNCs	Cu^{2+}	—	0.016 μM	101
AuNCs/Zn-MOF	AuNCs	Zn^{2+}	12.3 nM–24.6 μM	6 nM	102
CDs/AuNCs@ZIF-8	AuNCs	Hg^{2+}	800 nM–10 μM	77 pM	103
AuNCs/MIL-68(In)-NH$_2$/Cys	AuNCs	Hg^{2+}	20 pM–0.2 μM	6.7 pM	104
			0.2–60 μM		
MNPs/ATT-AuNCs@ZIF-8	AuNCs	Hg^{2+}	—	—	105
AgNCs/BPQDs/MOF	AgNCs	Baicalin	0.01–500 μM	3 ng mL^{-1}	106
ZIF-8@Pd NCs	Pd NCs	Glucose, cholesterol	—	0.10 μM	72
			—	0.092 μM	

Fig. 2 (A) Schematic of AuNCs@Zr-MOFs; (i) preparation of 2D AuNCs@Zr-MOF nanosheets, (ii) immobilization of the aptamer strands, and (iii) the detection of cocaine. (B) and (C) SEM and (D) and (E) HR-TEM images of 2D AuNCs@521-MOF nanosheets. (F) EIS diagrams of Apt/AuNCs@Zr-MOF/AE in the presence of various concentrations of cocaine (0, 0.001, 0.005, 0.01, 0.05, 0.1, 0.5, and 1.0 ng mL^{-1}). (G) Plot of ΔR_{ct} increase $vs.$ logarithm of the added cocaine concentrations. Reproduced with permission from the American Chemical Society.[107]

and covalent bonding between the oligonucleotide and the AuNCs@Zr-MOF framework.

The TEM and SEM images of AuNCs@Zr-MOF in Fig. 2 showcase a hierarchical nanoflower-like structure formed by the self-assembly of randomly oriented nanosheets. These nanoflowers, with diameters between 2.5 and 4.0 μm, are composed of nanosheets that are approximately 350 nm thick. HR-TEM images reveal aggregated nanosheets containing numerous embedded Au nanoclusters (NCs), which are approximately 2.0 nm in size. The lattice spacing of these Au NCs is

around 0.23 nm, aligning with the (111) lattice plane of gold. Electrochemical impedance spectroscopy (EIS) and differential pulse voltammetry (DPV) were employed for the analytical measurements. Different concentrations were then introduced into the electrochemical measurement system (Fig. 2F). Notably, the increase in ΔR_{ct} $versus$ the logarithmic plot of various cocaine concentrations demonstrated a linear range between 0.001 and 1.0 ng mL^{-1} (Fig. 2G). The AuNCs@Zr-MOF probe showed a high sensitivity for detecting cocaine within a wide concentration range of 0.001–1.0 ng mL^{-1}, and the LOD of 1.29 pM and 2.22 pM, as

determined by electrochemical impedance spectroscopy and differential pulse voltammetry, respectively.

In another work, Li et al.[102] prepared the AuNCs@Zn-MOF nanocomposite *via in situ* method for use in a fluorescence turn-on mechanism for the detection of zinc ions (Fig. 3A). Glutathione-capped AuNCs (GSH-AuNCs) were prepared *via* the reduction of Au^{3+} ions by glutathione as reducing and capping agents. They reported on the *in situ* formation of AuNCs@ Zn-MOF with the observed aggregation-induced emission enhancement (AIEE) in an aqueous media. The fluorescence quantum yield (QY) of Au NCs@Zn-MOF was 36.6%, which was nearly 9 times that of the AuNCs alone due to the aggregation, as claimed by Li and coworkers.[102]

Fig. 3B shows the spherical shape GSH-AuNCs with a diameter of about 2–3 nm and good dispersion. The prepared AuNCs displayed no surface plasmon resonance at around 520 nm (Fig. 3C), suggesting the formation of AuNCs with a diameter of less than 5 nm. Fig. 3D shows the fluorescence emission of GSH-AuNCs, with a peak emission at 570 nm when excited at 410 nm. Under UV light at 365 nm, the GSH-AuNCs exhibit a strong orange fluorescence (inset of Fig. 3D), and the quantum yield (QY) is calculated to be 4.1%. The fluorescence intensity of the GSH-AuNCs is increased significantly within Zn-MOF, as shown in Fig. 3E. Conversely, control experiments conducted without the MOF precursors, such as 2-MIM or Zn^{2+} ions, exhibit negligible changes in fluorescence. This fluorescence enhancement of the AuNCs is likely a result of Zn-MOF formation.

In addition to the red AuNCs, blue-emitting AuNCs were prepared and used. Red Eu-based MOF with blue-emitting AuNCs were integrated for ratiometric fluorescence and visual sensing of ATP by Zhou et al.[97]

The addition of ATP leads to the decomposition of Eu-MOF due to the strong affinity of Eu^{3+} with ATP (Fig. 4A). Hence, a ratiometric platform was obtained and the red emission of Eu-MOF decreases, while the blue emission of AuNCs remains unchanged. The AuNCs@Eu-MOF nanocomposite was prepared
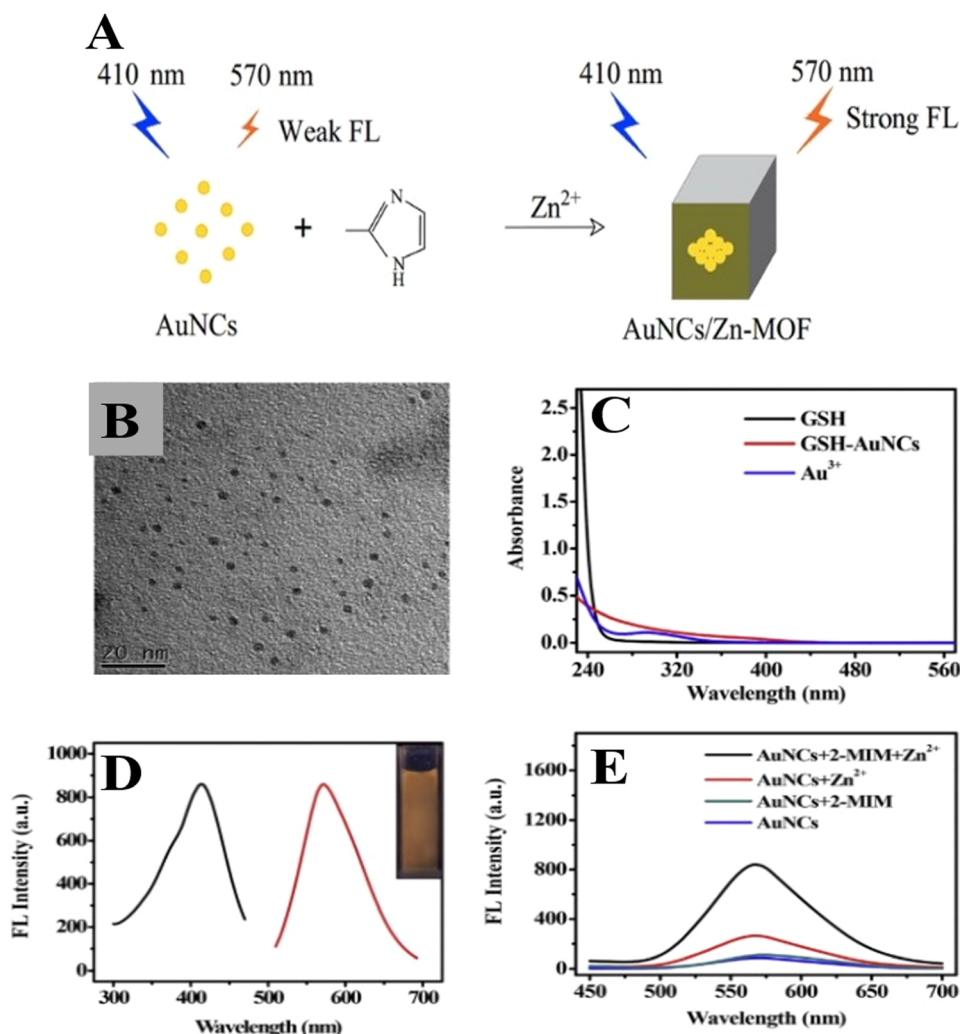

Fig. 3 (A) Preparation scheme for the AuNCs@Zn-MOF nanocomposite. (B) TEM digital micrograph of GSH-AuNCs. (C) Absorption of GSH (black line), GSH-AuNCs (red line) and Au^{3+} (blue line). (D) Excitation (black line) and emission (red line) spectra of GSH-AuNCs; inset: photograph of the GSH-AuNCs solution under UV light at 365 nm. (E) FL spectra of GSH-AuNCs (in 0.01 M HAc–NaAc buffer) coexisting with 0.43 mM 2-MIM and 12.3 mM Zn^{2+} (black line); 0.43 mM 2-MIM (dark cyan line); 12.3 mM Zn^{2+} (red line); nothing (blue line). Reproduced with permission from the American Chemical Society.[102]
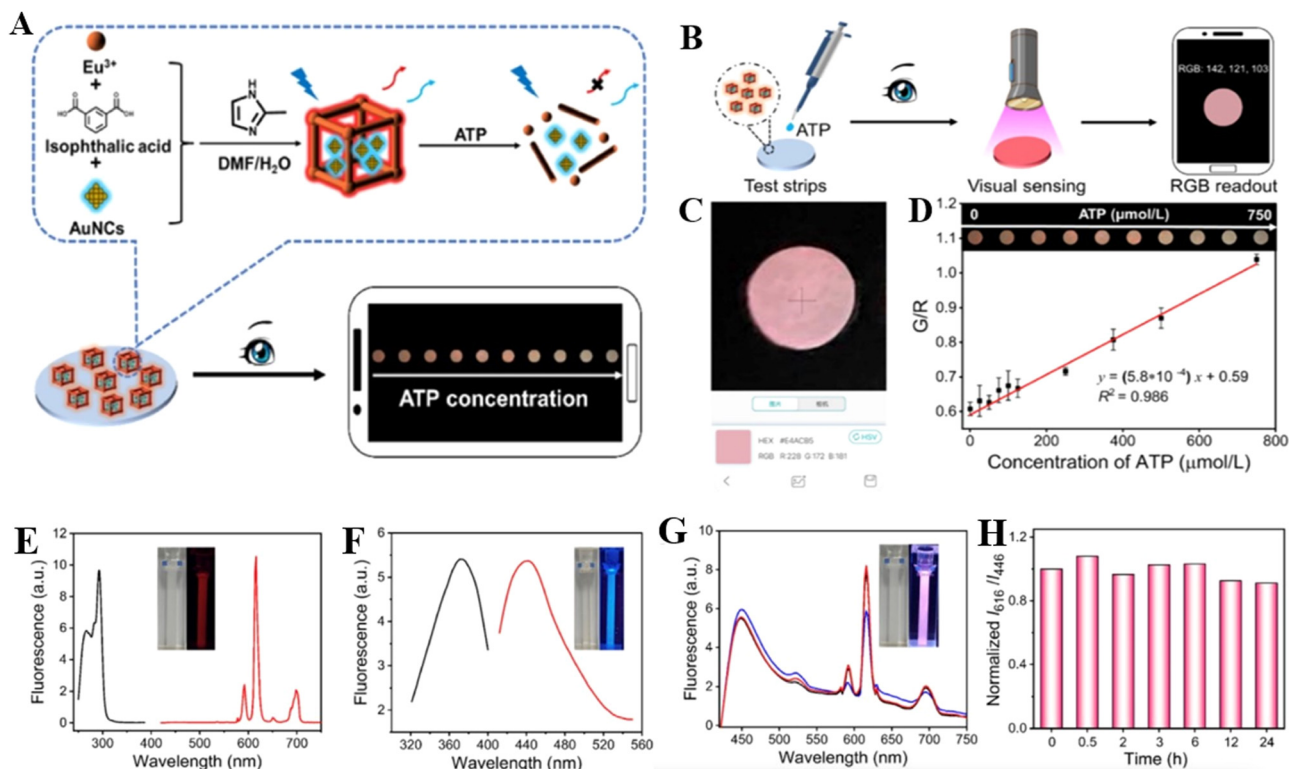
Fig. 4 (A) Illustration of the preparation process for the AuNCs@Eu-MOF nanocomposite. (B) Representation of ATP detection using a smartphone. (C) Image of a smartphone equipped with a color recognition app. (D) Color change of test strips (green channel/red channel) in response to varying ATP concentrations (insets display the photographs taken under a 310 nm UV lamp using a smartphone). (E) Excitation spectrum (black) and emission spectrum (red) of Eu-MOF; (F) BSA-AuNCs in aqueous solution; (G) fluorescence emission spectra of AuNCs@Eu-MOF with different molar ratios of AuNCs to Eu^{3+}: 80 : 1 (blue), 40 : 1 (red), and 20 : 1 (black); (H) fluorescence stability of AuNCs@Eu-MOF (40 : 1) *versus* the time in the aqueous solution. Excitation wavelength: 365 nm. Reproduced with permission from Elsevier.[97]

through self-assembly using Eu^{3+} ions and isophthalic acid as the precursors of MOF in the presence of bovine serum albumin-AuNCs (BSA-AuNCs).

The AuNCs@EuMOF platform demonstrated its effectiveness in solution, prompting further exploration into on-site ATP detection, with the material applied to paper (Fig. 4B). When ATP solution droplets were added to the test strips, the color of the paper spots shifted from pink to light blue under UV light as the ATP concentration increased from 0 to 750 µmol L^{-1}. To assess the ATP levels, RGB values from the paper sensor were recorded using a smartphone app (Fig. 4C). Fig. 4D shows a strong linear relationship ($R^2 = 0.986$) between the ratio of the green-to-red channel and ATP concentration, ranging from 25 to 750 µmol L^{-1}. These results indicate that the AuNCs@EuMOF on the test paper allows for portable, quantitative ATP detection with the simple use of a smartphone.

As a control experiment, BSA-AuNCs exhibit strong blue fluorescence with the emission peak at 446 nm, and Eu-MOF exhibits the characteristic red emission of Eu^{3+} with the emission peak at 616 nm owing to the antenna effect (Fig. 4E and F).

As depicted in Fig. 4G, the emission spectrum of AuNCs@Eu-MOF reveals peaks associated with both BSA-AuNCs and Eu^{3+}. Interestingly, the intensity of the dual emission was significantly influenced by the ratio of AuNCs to Eu^{3+}, with

the intensity ratio of Eu-MOF to AuNCs (I_{616}/I_{446}) reaching its peak at a 40 : 1 ratio. When the concentration of AuNCs was increased during synthesis, a slight decline in the emission band of Eu-MOF was observed, likely due to the coordination of carboxylate groups in BSA-AuNCs with the Eu^{3+} centers. Additionally, the researchers evaluated the fluorescence stability of AuNCs@Eu-MOF in aqueous solutions. The fluorescence intensity in Tris–HCl (pH 7.4) remained relatively stable over a 24-hour period, demonstrating good stability, as shown in Fig. 4H.

A surface modification strategy was employed to effectively adjust the NIR fluorescence properties of AuNCs by leveraging the beneficial attributes of ZIF-8.[81] The resulting AuNCs@ZIF-8 composites exhibited enhanced NIR fluorescence intensity at 830 nm, which is 190 nm longer than the emission wavelength of AuNCs without ZIF-8 encapsulation. Experimental results indicated that the long-wavelength emission arises from a ligand–metal charge transfer process in AuNCs, which is attributed to the confinement effect. By incorporating Rhodamine B into NIR-emitting AuNCs@ZIF-8 nanocomposites, a ratiometric fluorescent sensing platform was designed for detecting acetylcholinesterase (AChE). This sensing platform exploits the fluorescence increase of AuNCs in response to thiolates. The AuNCs@ZIF-8/RhB platform provides high sensitivity with a

detection limit of 0.4 mU mL^{-1}, and demonstrates strong specificity against typical biological interferences.

4.2. CuNCs@MOFs

CuNCs are gaining attention in biochemical sensing due to their distinct optical, catalytic, and electronic properties. Composed of only a few atoms, CuNCs exhibit strong, size-dependent fluorescence and excellent biocompatibility, which enhances their sensitivity in detecting biomolecules. They also offer cost-effective alternatives to noble metals like gold and silver, while maintaining high efficiency in biosensing applications.[108] These nanoclusters are used to detect various biological targets, including DNA, proteins, and metal ions, through fluorescence or catalytic signal amplification. Advances in stabilizing CuNCs in different environments have further broadened their applications in biochemical sensing and diagnostics.

Rogach *et al.*[71] prepared and encapsulated CuNCs into MOF to enhance the stability and emission intensity (Fig. 5A). The prepared CuNCs@MOF was utilized for the detection of trinitrotoluene, with the CuNCs being uniformly dispersed across the entire MOF structure. As shown in Fig. 5B, the TEM image reveals that the CuNCs are highly uniform in size, with a diameter of less than 2 nm, and exhibit a near-monodisperse distribution. The CuNC@ZIF-8 nanocomposite particles are also monodisperse but with smaller size, with an average diameter of 80 nm, as shown in the TEM image in Fig. 5C.

Fig. 5 (A) Schematic of the synthesis of Cu NC/ZIF-8 composites from Zn^{2+} ions, 2 MIm and Cu NCs. (B) TEM image of CuNC. (C) TEM image of CuNC@ZIF-8. (D) Photoluminescence spectrum (red) excited at 365 nm and excitation spectrum (black) with a detection wavelength of 600 nm of CuNCs (dotted lines) and CuNC@ZIF-8 (solid lines). Inset shows a photograph of light-emitting solutions containing Cu NCs (left cuvette) and CuNC@ZIF-8 composites (right cuvette). (E) Fluorescence decays of CuNCs (black) and CuNC@ZIF-8 composites (red); (F) relative fluorescence intensity (at 600 nm) of CuNCs after different storage times (hours) as compared to (G) the fluorescence intensity of the CuNC@ZIF-8 composites (stored for days). Reproduced with permission from Wiley-VCH GmbH.[71]

The CuNC@ZIF-8 composites exhibit a strong emission peak at 600 nm (orange emission, as indicated in the inset of Fig. 5D), contrasting with the weak red emission at 620 nm seen in the bare CuNCs. This blue shift in the emission of CuNCs upon their incorporation into ZIF-8 is attributed to the enhanced inter-Cu interactions relative to the intra-Cu
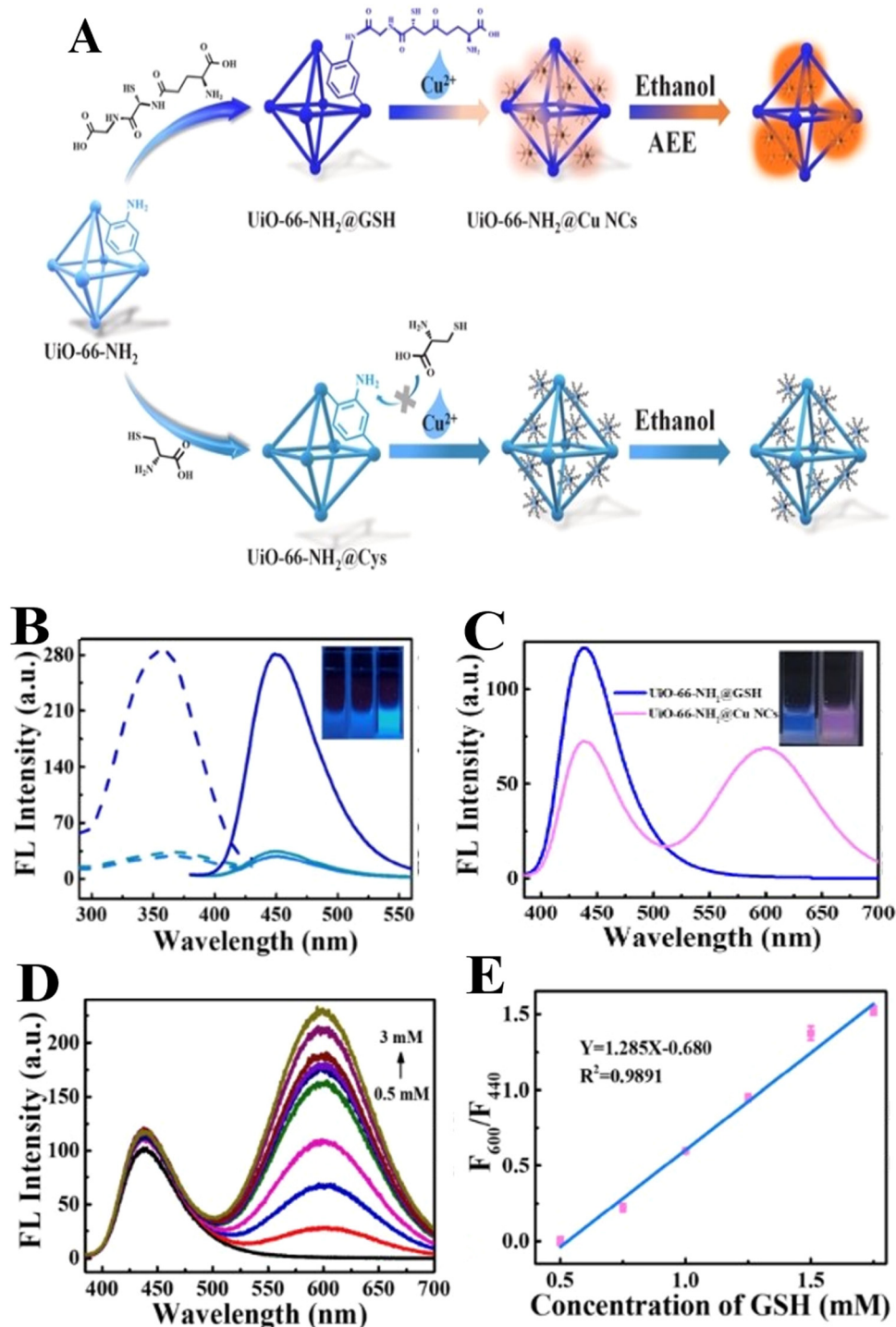

Fig. 6 (A) Schematic depicting the selective discrimination between GSH and Cys, utilizing UiO-66-NH$_2$ and UiO-66-NH$_2$@CuNCs as the detection platforms. (B) Excitation (dotted line, λ_{em} = 450 nm) and fluorescence (solid line) spectra of UiO-66-NH$_2$ (shallow blue line), in the presence of GSH (blue line) and Cys (cyan line), with the photographs under UV light shown as the inset. (C) Emission spectra of UiO-66-NH$_2$@GSH (blue line) and UiO-66-NH$_2$@CuNCs (pink line), after injection into ethanol, with their photographs under 365 nm UV light shown in the inset. (D) Fluorescence spectra of UiO-66-NH$_2$@CuNCs on addition of different concentrations of GSH. (E) Calibration curve of UiO-66-NH$_2$@CuNCs vs. different concentrations of GSH. Reproduced with permission from Elsevier.[82]

interactions within the clusters, leading to an increase in the average distance between Cu(I) ions.

This aligns with the positions of the fluorescence excitation spectra for both bare and CuNCs@MOF, as depicted in Fig. 5E. The fluorescence quantum yield (QY) increased by over 20-fold, rising from 0.5% for CuNCs to 11% for Cu NC@ZIF-8 composites. The average fluorescence lifetime increased significantly from 1.3 μs for the bare CuNCs to 11.1 μs after the clusters were incorporated into the ZIF-8 framework.

The CuNCs stability is very important for various applications. As depicted in Fig. 5F and G, the fluorescence intensity of pure CuNCs rapidly declines under ambient conditions, with a reduction of over 50% in just 5 hours. In contrast, CuNC@ZIF-8 shows only a minor decrease (less than 15%) in fluorescence intensity even after two weeks of storage. This enhanced stability is attributed to the protective effect of ZIF-8, which reduces the likelihood of oxidation of the metal core in the clusters. Finally, they used CuNC/ZIF-8 composites as luminescent probes for detecting TNT, an explosive and environmental pollutant. The emission of these composites is selectively quenched by even small amounts of TNT. The PL quenching occurs within 15 minutes and remains stable with minimal fluctuation over a 2-hour period. The quantitative concentration range of TNT was 5 to 80×10^{-6} M and the LOD was 8.5×10^{-6} M.

A ratiometric platform was designed for the detection of glutathione (GSH) based on CuNCs@UiO-66-NH$_2$.[82] The ratiometric assay was capable of discriminating and detecting GSH and Cys.

The initial weak fluorescence of UiO-66-NH$_2$ was significantly intensified after its reaction with GSH, as a result of the rotation-restricted emission enhancement mechanism. Moreover, the GSH-activated UiO-66-NH$_2$ was used as both a template and a reducing agent in the synthesis of orange-red aggregation-induced emission (AEE)-active CuNC composites (UiO-66-NH$_2$@Cu NCs), as depicted in Fig. 6A. This highlights the dual functionality of UiO-66-NH$_2$ in facilitating the formation of highly emissive CuNCs.

The introduction of GSH into the UiO-66-NH$_2$ structure caused a significant 10-fold increase in fluorescence intensity, particularly with enhanced excitation at 350 nm (Fig. 6B). In comparison, the addition of Cys led to only a two-fold increase, and the difference between the effects of GSH and Cys was clearly visible under 365 nm UV light (Fig. 2a inset). This suggests that the fluorescence enhancement at 450 nm is closely associated with the interaction between GSH and the amino groups on UiO-66-NH$_2$.

Addition of Cu^{2+} led to a new emission band at 600 nm, along with the original blue emission of UiO-66-NH$_2$@GSH at 450 nm (Fig. 6C).

As the concentration of GSH increased, the luminescence intensity at 600 nm steadily rose, while there was only a slight variation at 440 nm (Fig. 6E). A linear correlation between the ratio and GSH concentration was noted within the 0.5–1.75 mM range (Fig. 6F), with LOD for UiO-66-NH$_2$@CuNCs being established at 0.14 mM.

4.3. AgNCs@MOFs

Silver nanoclusters (AgNCs) are nanoscale aggregates of silver atoms, typically less than 2 nanometers in diameter, exhibiting unique optoelectronic properties due to quantum confinement effects. They demonstrate strong photoluminescence, remarkable catalytic activity, and antibacterial properties, making them valuable in applications such as bioimaging, sensing, and nanomedicine.[109] The stability and reactivity of AgNCs are
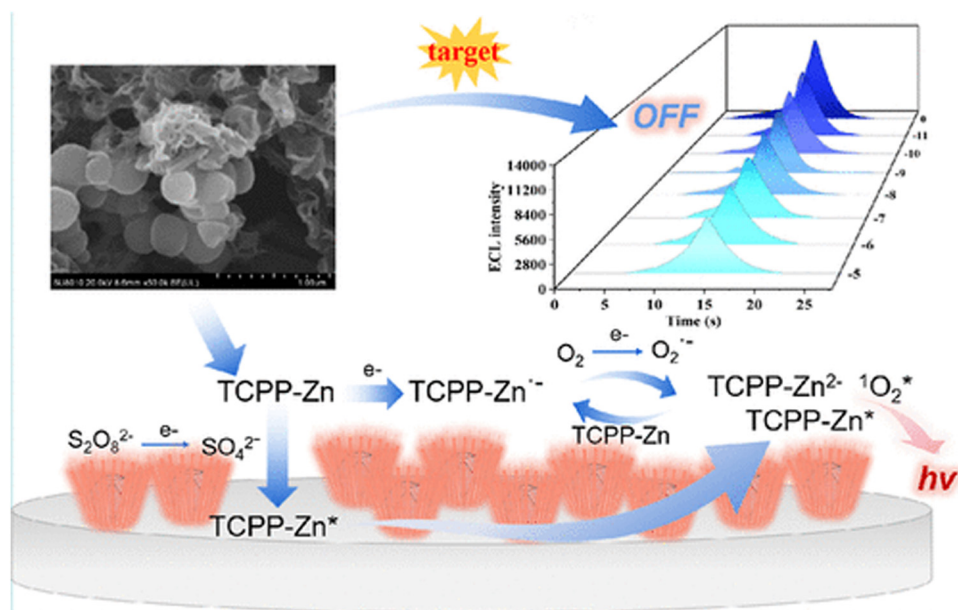

Fig. 7 Preparation and application of GSH–AgNCs–ZIF-8 in an ECL-based probe for the detection of iodide ions. Reproduced with permission from the American Chemical Society.[110]

influenced by their size, structure, and the organic ligands used during synthesis.

Chang *et al.*[110] synthesized ZIF-8 and glutathione silver nanoclusters (GSH-AgNCs) *in situ* to form a composite material (GSH-AgNCs-ZIF-8), as shown in Fig. 7. Additionally, a luminescent functional assembly of nanocomposites was achieved by innovatively mixing the luminophores tetracarboxyphenyl zinc porphyrin (TCPP-Zn) with GSH-AgNCs-ZIF-8, resulting in adjustable luminescence properties. The resulting composite served as a highly efficient luminophore for constructing an electrochemiluminescence (ECL) sensing system for the detection of iodide ions (I⁻), with an in-depth investigation of the ECL mechanism. The ECL-based sensors demonstrated excellent responsiveness to I⁻ within a linear range of 10 pM to 10 μM, exhibiting selectivity, stability, and sensitivity.

4.4 PdNCs@MOFs

A composite comprising 1.5 nm of PdNCs confined in the matrix od ZIF-8 was prepared successfully by Li *et al.*[72] PdNCs@ZIF-8 was used as a peroxidase-like nanozyme for

the fluorescent detection of glucose and cholesterol using both glucose oxidase and cholesterol oxidase, respectively (Fig. 8A).

The FE-SEM images (Fig. 8B) illustrate that Pd@ZIF-8 possesses a distinct dodecahedral structure, with an average particle size of around 150 ± 20 nm. Additionally, the PXRD spectra shown in Fig. 8C confirm that the diffraction peaks of the synthesized ZIF-8 are in perfect alignment with those of the simulated ZIF-8, verifying that the material's high crystallinity remains intact even after the incorporation of Pd nanoclusters. This consistency underscores the stability of the ZIF-8 framework during the Pd loading process. The absence of characteristic diffraction peaks for metallic Pd suggests that the Pd nanoclusters are highly dispersed within the ZIF-8 framework. Fig. 8D shows the TEM images of the PdNCs size in Pd@ZIF-8. A fluorescent sensing platform was constructed using the PdNCs@ZIF-8 nanocomposite and thiamine as a fluorogenic substrate. A detection linearity of 5 to 1000 μM and LOD about 0.9 μM were achieved (Fig. 8B).
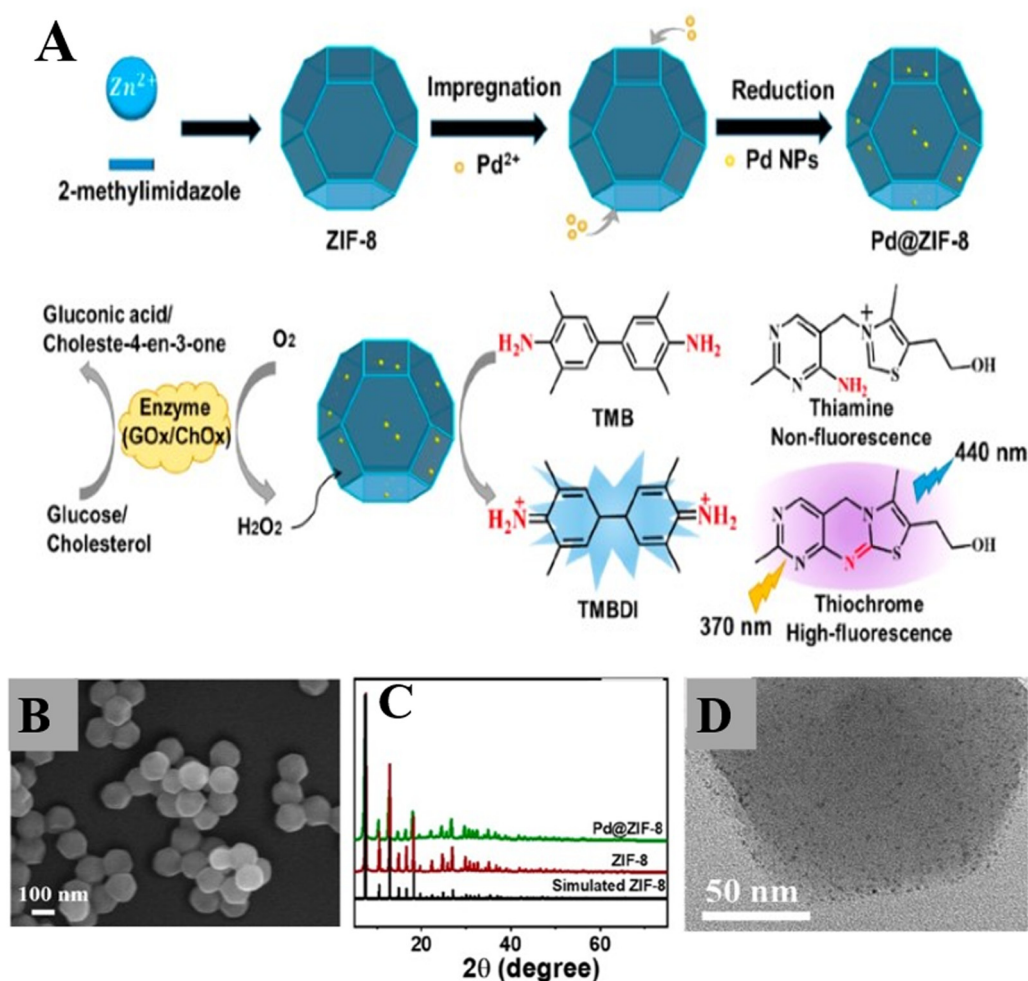

Fig. 8 (A) Schematic of the synthesis of Pd@ZIF-8 and its peroxidase-like activity for the detection of H_2O_2, cholesterol, and glucose (bottom row). (B) SEM image of Pd@ZIF-8. (C) XRD patterns of simulated ZIF-8, ZIF-8, and Pd@ZIF-8. (D) TEM image of Pd@ZIF-8 nanocomposite. Reproduced with permission from the American Chemical Society.[72]

5. Conclusions and future perspectives

The integration of atomically precise NCs with MOFs has gained significant attention as a groundbreaking strategy in the development of next-generation materials for biochemical sensing applications. This approach exploits the complementary properties of both materials, not only enhancing their performance and functionality, but also overcoming the individual drawbacks that each material exhibits when used alone. NCs are known for their high fluorescence quantum yield, exceptional catalytic activity, and quantum-size effects, which contribute to highly sensitive and efficient detection processes. When integrated with MOFs, which are characterized by their tunable pore structures, excellent stability, and selective binding capabilities, the resulting NC@MOF composites exhibit remarkable improvements in sensing performance. Specifically, the incorporation of NCs within the robust framework of MOFs not only preserves the NCs' unique properties, but also enhances the overall stability and selectivity of the sensor. The synergy between NCs and MOFs leads to superior sensitivity, selectivity, and stability in detecting target analytes, making these composites highly effective for a wide range of biochemical sensing applications. This integrated approach represents a promising pathway for the development of more efficient, reliable, and versatile sensing platforms for environmental monitoring, healthcare diagnostics, and other critical applications.

One of the key challenges moving forward is enhancing the emission properties of NCs when embedded within MOFs. Achieving stronger and more stable luminescence will open new avenues for NC@MOF applications in fluorescence-based sensing and imaging. Strategies to boost the emission include optimizing the spatial confinement of NCs within the MOF matrix, fine-tuning the interaction between NCs and MOF ligands, and engineering the MOF structure to minimize quenching effects, while maintaining strong NC-MOF coupling. Moreover, improving the stability of NCs within MOFs—particularly under harsh environmental conditions—is crucial for extending the lifespan of these sensors. Developing MOF structures that provide robust protection against NC aggregation and thermal degradation will be essential to ensure consistent performance.

In biochemical sensing, selectivity poses another critical challenge. The ability of NC@MOFs to distinguish specific analytes, especially in complex biological matrices, depends on the precise tailoring of MOF structures and functional groups. Introducing selective binding sites or ligand modifications within MOFs can enhance the specificity for target molecules, while reducing interference from other species. This dual focus on improving luminescence properties and selectivity is essential for advancing NC@MOF-based sensors for biochemical applications.

Looking ahead, future research should focus on further expanding the functionality of NC@MOF composites to unlock their full potential. One promising direction involves the integration of additional functional groups or dopants into the MOF component, which would enhance their selectivity and sensitivity toward specific target analytes. By tailoring the MOF's properties, it would be possible to create highly specialized sensors capable of detecting a wide variety of substances with increased precision. Moreover, there is significant potential in designing multifunctional NC@MOF composites that can simultaneously perform dual or even triple roles in various applications, such as sensing, catalysis, and therapeutic delivery. This would broaden the scope of their use in complex systems, making them more versatile and efficient. Additionally, exploring dynamic MOF structures that respond to external stimuli—such as changes in temperature, pH, or light—could further increase the adaptability of these composites. These responsive systems could be fine-tuned to react to environmental or biological signals, thereby enhancing their utility in diverse biochemical and environmental sensing applications. With such innovations, NC@MOF composites could become essential tools in the development of advanced sensing technologies, offering new capabilities and addressing challenges across a variety of fields.

In summary, the NC@MOF composite platform holds immense potential for next-generation sensor technologies. Future work focusing on optimizing the emission properties, stability, and multifunctionality will be key to unlocking the full capabilities of these hybrid materials, driving their adoption in commercial applications and expanding their role in catalysis, energy, and biomedical fields.

Data availability

All raw data and results that support the findings of this study are available from the corresponding author upon request.

Conflicts of interest

The authors declare no competing financial interest.

References

1 F. Mustafa and S. Andreescu, Nanotechnology-based approaches for food sensing and packaging applications, *RSC Adv.*, 2020, **10**, 19309–19336, DOI: **10.1039/D0RA01084G**.

2 S. Shrivastava and D. Dash, Applying Nanotechnology to Human Health: Revolution in Biomedical Sciences, *J. Nanotechnol.*, 2009, **2009**, 184702, DOI: **10.1155/2009/184702**.

3 S. Moradi, A. Firoozbakhtian, M. Hosseini, O. Karaman, S. Kalikeri, G. G. Raja and H. Karimi-Maleh, Advancements in wearable technology for monitoring lactate levels using lactate oxidase enzyme and free enzyme as analytical approaches: a review, *Int. J. Biol. Macromol.*, 2024, **254**, 127577, DOI: **10.1016/j.ijbiomac.2023.127577**.

4 S. S. Mohammed Ameen, F. Algethami and K. M. Omer, Pine needle-derived oxidase-like Mn nanozymes: sustainable nanozyme, scalable synthesis, and visual and colorimetric

nitrite detection, *Microchim. Acta*, 2025, **192**, 146, DOI: **10.1007/s00604-025-07024-0**.

5 Y. Han, P. Zhang, X. Duan, X. Gao and L. Gao, Advances in precise synthesis of metal nanoclusters and their applications in electrochemical biosensing of disease biomarkers, *Nanoscale*, 2025, **17**, 3616–3634, DOI: **10.1039/D4NR04714A**.

6 H. Nasrollahpour, B. J. Sánchez, M. Sillanpää and R. Moradi, Metal nanoclusters in point-of-care sensing and biosensing applications, *ACS Appl. Nano Mater.*, 2023, **6**, 12609–12672, DOI: **10.1021/acsanm.3c01569**.

7 S. Qian, Z. Wang, Z. Zuo, X. Wang, Q. Wang and X. Yuan, Engineering luminescent metal nanoclusters for sensing applications, *Coord. Chem. Rev.*, 2022, **451**, 214268, DOI: **10.1016/j.ccr.2021.214268**.

8 L. Shang, J. Xu and G. U. Nienhaus, Recent advances in synthesizing metal nanocluster-based nanocomposites for application in sensing, imaging and catalysis, *Nano Today*, 2019, **28**, 100767.

9 F. Bazzi, M. Hosseini, B. Ebrahimi-Hoseinzadeh, H. A. J. Al Lawati and M. R. Ganjali, A dual-targeting nanobiosensor for Gender Determination applying Signal Amplification Methods and integrating Fluorometric Gold and Silver Nanoclusters, *Microchim. Acta*, 2023, **190**, 368, DOI: **10.1007/s00604-023-05947-0**.

10 A. B. Pebdeni, M. Mousavizadegan and M. Hosseini, Sensitive detection of *S. aureus* using aptamer-and vancomycin-copper nanoclusters as dual recognition strategy, *Food Chem.*, 2021, **361**, 130137, DOI: **10.1016/j.foodchem.2021.130137**.

11 A. Bahmani, E. Shokri, M. Hosseini and S. Hosseinkhani, A fluorescent aptasensor based on copper nanoclusters for optical detection of CD44 exon v10, an important isoform in metastatic breast cancer, *Anal. Methods*, 2021, **13**, 3837–3844, DOI: **10.1039/d1ay01087e**.

12 A. Longo, E. J. J. de Boed, N. Mammen, M. van der Linden, K. Honkala, H. Häkkinen, P. E. de Jongh and B. Donoeva, Towards Atomically Precise Supported Catalysts from Monolayer-Protected Clusters: The Critical Role of the Support, *Chem. – Eur. J.*, 2020, **26**, 7051–7058, DOI: **10.1002/chem.202000637**.

13 Z. Yan, M. G. Taylor, A. Mascareno and G. Mpourmpakis, Size-, Shape-, and Composition-Dependent Model for Metal Nanoparticle Stability Prediction, *Nano Lett.*, 2018, **18**, 2696–2704, DOI: **10.1021/acs.nanolett.8b00670**.

14 T. Islamoglu, Z. Chen, M. C. Wasson, C. T. Buru, K. O. Kirlikovali, U. Afrin, M. R. Mian and O. K. Farha, Metal–Organic Frameworks against Toxic Chemicals, *Chem. Rev.*, 2020, **120**, 8130–8160, DOI: **10.1021/acs.chemrev.9b00828**.

15 A. J. Howarth, Y. Liu, P. Li, Z. Li, T. C. Wang, J. T. Hupp and O. K. Farha, Chemical, thermal and mechanical stabilities of metal–organic frameworks, *Nat. Rev. Mater.*, 2016, **1**, 15018, DOI: **10.1038/natrevmats.2015.18**.

16 L. E. Kreno, K. Leong, O. K. Farha, M. Allendorf, R. P. Van Duyne and J. T. Hupp, Metal–organic framework materials as chemical sensors, *Chem. Rev.*, 2012, **112**, 1105–1125, DOI: **10.1021/cr200324t**.

17 S. S. Mohammed Ameen, A. Bedair, M. Hamed, F. R. Mansour and K. M. Omer, Recent Advances in Metal–Organic Frameworks as Oxidase Mimics: A Comprehensive Review on Rational Design and Modification for Enhanced Sensing Applications, *ACS Appl. Mater. Interfaces*, 2024, **17**, 110–129, DOI: **10.1021/acsami.4c17397**.

18 A. Karrat, J. Benssbihe, S. S. M. Ameen, K. M. Omer and A. Amine, Development of a Silver-Based MOF Oxidase-Like nanozyme modified with molecularly imprinted polymers for sensitive and selective colorimetric detection of quercetin, *Spectrochim. Acta, Part A*, 2025, 125735, DOI: **10.1016/j.saa.2025.125735**.

19 S. S. Mohammed Ameen and K. M. Omer, Lanthanide and functionalization-free dual-state emitting zinc-based MOFs followed by dual-state detection: ratiometric and color-tonality visual detection of tetracycline in solution and on paper in food and environmental samples, *Microchim. Acta*, 2025, **192**, 22, DOI: **10.1007/s00604-024-06896-y**.

20 S. S. M. Ameen, N. M. S. Mohammed and K. M. Omer, Visual monitoring of silver ions and cysteine using bi-ligand Eu-based metal organic framework as a reference signal: color tonality, *Microchem. J.*, 2022, **181**, 107721, DOI: **10.1016/j.microc.2022.107721**.

21 P. B. Hassan, S. S. M. Ameen, L. Mohammed, S. M. M. Ameen and K. M. Omer, Enhanced antibacterial activity of a novel silver-based metal organic framework towards multidrug-resistant *Klebsiella pneumonia*, *Nanoscale Adv.*, 2024, **6**, 3801–3808, DOI: **10.1039/D4NA00037D**.

22 S. S. M. Ameen and K. M. Omer, Recent Advances of Bimetallic-Metal Organic Frameworks: Preparation, Properties, and Fluorescence-Based Biochemical Sensing Applications, *ACS Appl. Mater. Interfaces*, 2024, **16**, 31895–31921, DOI: **10.1021/acsami.4c06931**.

23 M. Wu, Z. W. Jiang, P. Zhang, X. Gong and Y. Wang, Energy transfer-based ratiometric fluorescence sensing anthrax biomarkers in bimetallic lanthanide metal–organic frameworks, *Sens. Actuators, B*, 2023, **383**, 133596, DOI: **10.1016/j.snb.2023.133596**.

24 Y. Songlin, S. Dongxue, L. Kaisu, W. Lei, Z. Ying, S. Yaguang, Z. Mingchang and W. Shuangyan, Synthesis of a lanthanide-based bimetallic-metal–organic framework for luminescence sensing anthrax biomarker, *Dyes Pigm.*, 2023, **220**, 111673, DOI: **10.1016/j.dyepig.2023.111673**.

25 Z. Zhao, S. Yang, M. Zhu, Y. Zhang, Y. Sun and S. Wu, A multicenter lanthanide coordination polymer for ratiometric pesticide monitoring, *Sens. Actuators, B*, 2023, **383**, 133593, DOI: **10.1016/j.snb.2023.133593**.

26 X. Yue, L. Fu, Y. Li, S. Xu, X. Lin and Y. Bai, Lanthanide bimetallic MOF-based fluorescent sensor for sensitive and visual detection of sulfamerazine and malachite, *Food Chem.*, 2023, **410**, 135390, DOI: **10.1016/j.foodchem.2023.135390**.

27 L. Yu, Q. Zheng, D. Wu and Y. Xiao, Bimetal–organic framework nanocomposite based point-of-care visual ratiometric fluorescence pH microsensor for strong acidity, *Sens. Actuators, B*, 2019, **294**, 199–205, DOI: **10.1016/j.snb.2019.05.037**.

28 J. M. Gonçalves, P. R. Martins, D. P. Rocha, T. A. Matias, M. S. S. Juliao, R. A. A. Munoz and L. Angnes, Recent trends

and perspectives in electrochemical sensors based on MOF-derived materials, *J. Mater. Chem. C*, 2021, **9**, 8718–8745.

29 I. B. Qader, S. S. M. Ameen, H. A. Qader and K. M. Omer, Visual-Based Platform Using Sustainable Intrinsic Fluorescent Zn-Based Metal–Organic Framework for Detection of Folic Acid in Pharmaceutical Formulations, *J. Inorg. Organomet. Polym. Mater.*, 2024, 1–10, DOI: **10.1007/s10904-024-03322-x**.

30 S. S. M. Ameen, I. B. Qader, H. A. Qader, F. K. Algethami, B. Y. Abdulkhair and K. M. Omer, Dual-state dual emission from precise chemically engineered bi-ligand MOF free from encapsulation and functionalization with self-calibration model for visual detection, *Microchim. Acta*, 2024, **191**, 62, DOI: **10.1007/s00604-023-06148-5**.

31 Y. Zhai, Y. Li, X. Huang, J. Hou, H. Li and S. Ai, Colorimetric and ratiometric fluorescent dual-mode sensitive detection of Hg^{2+} based on UiO-66-NH2@ Au composite, *Spectrochim. Acta, Part A*, 2022, **275**, 121187, DOI: **10.1016/j.saa.2022.121187**.

32 Y.-M. Li, J. Hu and M. Zhu, Confining atomically precise nanoclusters in metal–organic frameworks for advanced catalysis, *Coord. Chem. Rev.*, 2023, **495**, 215364.

33 A. Arenas-Vivo, S. Rojas, I. Ocaña, A. Torres, M. Liras, F. Salles, D. Arenas-Esteban, S. Bals, D. Ávila and P. Horcajada, Ultrafast reproducible synthesis of a Ag-nanocluster@ MOF composite and its superior visible-photocatalytic activity in batch and in continuous flow, *J. Mater. Chem. A*, 2021, **9**, 15704–15713.

34 S. M. Pirot and K. M. Omer, Surface imprinted polymer on dual emitting MOF functionalized with blue copper nanoclusters and yellow carbon dots as a highly specific ratiometric fluorescence probe for ascorbic acid, *Microchem. J.*, 2022, **182**, 107921, DOI: **10.1016/j.microc.2022.107921**.

35 S. M. Pirot and K. M. Omer, Designing of robust and sensitive assay via encapsulation of highly emissive and stable blue copper nanocluster into zeolitic imidazole framework (ZIF-8) with quantitative detection of tetracycline, *J. Anal. Sci. Technol.*, 2022, **13**, 22, DOI: **10.1186/s40543-022-00333-6**.

36 X.-R. Song, N. Goswami, H.-H. Yang and J. Xie, Functionalization of metal nanoclusters for biomedical applications, *Analyst*, 2016, **141**, 3126–3140.

37 E. Porret, X. Le Guével and J.-L. Coll, Gold nanoclusters for biomedical applications: toward in vivo studies, *J. Mater. Chem. B*, 2020, **8**, 2216–2232.

38 K. Liu, Z. Chen, T. Islamoglu, S.-J. Lee, H. Chen, T. Yildirim, O. K. Farha and R. Q. Snurr, Exploring the Chemical Space of Metal–Organic Frameworks with rht Topology for High Capacity Hydrogen Storage, *J. Phys. Chem. C*, 2024, **128**, 7435–7446, DOI: **10.1021/acs.jpcc.4c00638**.

39 J. Duncan, D. Sengupta, S. Bose, K. O. Kirlikovali and O. K. Farha, Defect-induced confinement in zirconium metal–organic frameworks for enhanced hydrogen adsorption, *Sustainable Chem. Environ.*, 2023, **3**, 100032, DOI: **10.1016/j.scenv.2023.100032**.

40 S. S. M. Ameen and K. M. Omer, Temperature-resilient and sustainable Mn-MOF oxidase-like nanozyme (UoZ-4) for total antioxidant capacity sensing in some citrus fruits: breaking the temperature barrier, *Food Chem.*, 2024, **448**, 139170, DOI: **10.1016/j.foodchem.2024.139170**.

41 S. S. Mohammed Ameen and K. M. Omer, Pushing Boundaries: Introducing Silver-Based Metal–Organic Framework Oxidase-Like Nanozyme over a Wide-Range Temperature, *ACS Appl. Nano Mater.*, 2024, **7**, 20793–20803, DOI: **10.1021/acsanm.4c03725**.

42 A. Bedair, M. Hamed, S. S. M. Ameen, K. M. Omer and F. R. Mansour, Polyphenolic antioxidant analysis using metal organic Frameworks: theoretical foundations and practical applications, *Microchem. J.*, 2024, **205**, 111183, DOI: **10.1016/j.microc.2024.111183**.

43 S. S. Mohammed Ameen and K. M. Omer, Merging Dual Antenna Effect with Target-Insensitive Behavior in Bimetal Biligand MOFs to Form Efficient Internal Reference Signal: Color Tonality-Ratiometric Designs, *ACS Mater. Lett.*, 2024, **6**, 2339–2349, DOI: **10.1021/acsmaterialslett.4c00845**.

44 S. S. M. Ameen and K. M. Omer, Multifunctional MOF: cold/hot adapted sustainable oxidase-like MOF nanozyme with ratiometric and color tonality for nitrite ions detection, *Food Chem.*, 2024, **462**, 141027, DOI: **10.1016/j.foodchem.2024.141027**.

45 B. Shi, X. Zhang, W. Li, N. Liang, X. Hu, J. Xiao, D. Wang, X. Zou and J. Shi, An intrinsic dual-emitting fluorescence sensing toward tetracycline with self-calibration model based on luminescent lanthanide-functionalized metal–organic frameworks, *Food Chem.*, 2023, **400**, 133995, DOI: **10.1016/j.foodchem.2022.133995**.

46 M. F. Sanad, A. R. P. Santiago, S. A. Tolba, A. Ahsan, O. Fernandez-delgado, M. S. Adly, E. M. Hashem, M. M. Abodouh, M. S. El-shall, S. T. Sreenivasan, N. K. Allam and L. Echegoyen, Co–Cu Bimetallic Metal Organic Framework Catalyst Outperforms the Pt/C Benchmark for Oxygen Reduction, *J. Am. Chem. Soc.*, 2021, **143**(10), 4064–4073, DOI: **10.1021/jacs.1c01096**.

47 N. Wu, H. Guo, X. Wang, L. Sun, T. Zhang, L. Peng and W. Yang, A water-stable lanthanide-MOF as a highly sensitive and selective luminescence sensor for detection of Fe^{3+} and benzaldehyde, *Colloids Surf., A*, 2021, **616**, 126093, DOI: **10.1016/j.colsurfa.2020.126093**.

48 C. Hon Lau, R. Babarao and M. R. Hill, A route to drastic increase of CO_2 uptake in Zr metal organic framework UiO-66, *Chem. Commun.*, 2013, **49**, 3634–3636, DOI: **10.1039/c3cc40470f**.

49 M. Ding, R. W. Flaig, H.-L. Jiang and O. M. Yaghi, Carbon capture and conversion using metal–organic frameworks and MOF-based materials, *Chem. Soc. Rev.*, 2019, **48**, 2783–2828, DOI: **10.1039/C8CS00829A**.

50 T. A. Goetjen, A. J. Kropf, S. Alayoglu, M. Delferro, J. T. Hupp and O. K. Farha, Tuning the Product Distribution of Acetylene Dimerization through Bimetallic Metal–Organic Framework-Supported Nanoporous Systems, *ACS Appl. Nano Mater.*, 2022, **5**, 14961–14969, DOI: **10.1021/acsanm.2c03201**.

51 K. Ma, Y. H. Cheung, H. Xie, X. Wang, M. Evangelopoulos, K. O. Kirlikovali, S. Su, X. Wang, C. A. Mirkin, J. H. Xin and O. K. Farha, Zirconium-Based Metal–Organic Frameworks as Reusable Antibacterial Peroxide Carriers for Protective Textiles, *Chem. Mater.*, 2023, **35**, 2342–2352, DOI: **10.1021/acs.chemmater.2c03288**.

52 H. Bin Luo, F. R. Lin, Z. Y. Liu, Y. R. Kong, K. B. Idrees, Y. Liu, Y. Zou, O. K. Farha and X. M. Ren, MOF-Polymer Mixed Matrix Membranes as Chemical Protective Layers for Solid-Phase Detoxification of Toxic Organophosphates, *ACS Appl. Mater. Interfaces*, 2022, **15**, 2933–2939, DOI: **10.1021/acsami.2c18691**.

53 M. Ameen, S. Sh and K. M. Omer, Three in one: coordination-induced emission for inherent fluorescent Al-MOF synthesis combined with inner filter effect@ aggregation-induced emission mechanisms for designing color tonality and ratiometric sensing platforms, *Microchim. Acta*, 2024, **191**, 1–11, DOI: **10.1007/s00604-024-06535-6**.

54 S. S. Mohammed Ameen and K. M. Omer, Dual-State Red-Emitting Zinc-Based MOF Accompanied by Dual-Mode and Dual-State Detection: Color Tonality Visual Mode for the Detection of Tetracycline, *ACS Appl. Mater. Interfaces*, 2024, **16**, 51376–51383, DOI: **10.1021/acsami.4c13115**.

55 S. H. Al-Jaf, S. S. Mohammed Ameen and K. M. Omer, A novel ratiometric design of microfluidic paper-based analytical device for the simultaneous detection of Cu^{2+} and Fe^{3+} in drinking water using a fluorescent MOF@tetracycline nanocomposite, *Lab Chip*, 2024, **24**, 2306–2316, DOI: **10.1039/d3lc01045g**.

56 Y.-Z. Chen, R. Zhang, L. Jiao and H.-L. Jiang, Metal–organic framework-derived porous materials for catalysis, *Coord. Chem. Rev.*, 2018, **362**, 1–23, DOI: **10.1016/j.ccr.2018.02.008**.

57 J. Liu, P. K. Thallapally, B. P. McGrail, D. R. Brown and J. Liu, Progress in adsorption-based CO_2 capture by metal–organic frameworks, *Chem. Soc. Rev.*, 2012, **41**, 2308–2322, DOI: **10.1039/C1CS15221A**.

58 P. Kumar, A. Deep and K. H. Kim, Metal organic frameworks for sensing applications, *TrAC, Trends Anal. Chem.*, 2015, **73**, 39–53, DOI: **10.1016/j.trac.2015.04.009**.

59 H. A. Qader, S. Sh Mohammed Ameen, I. B. Qader and K. M. Omer, Portable on–off visual-mode detection using intrinsic fluorescent zinc-based metal–organic framework for detection of diclofenac in pharmaceutical tablets, *Spectrochim. Acta, Part A*, 2024, **322**, 124791, DOI: **10.1016/j.saa.2024.124791**.

60 J.-J. Hu, K.-L. Xie, T.-Z. Xiong, M.-M. Wang, H.-R. Wen, Y. Peng and S.-J. Liu, Stable Europium(III) Metal–Organic Framework Demonstrating High Proton Conductivity and Fluorescence Detection of Tetracyclines, *Inorg. Chem.*, 2023, **62**, 12001–12008.

61 H. Wan, Y. Wang, J. Chen, H.-M. Meng and Z. Li, 2D Co-MOF nanosheet-based nanozyme with ultrahigh peroxidase catalytic activity for detection of biomolecules in human serum samples, *Microchim. Acta*, 2021, **188**, 1–8.

62 L. Tian, C. Cheng, Z. Zhao, W. Liu and L. Qi, Enhancing the catalytic performance of MOF-polymer@AuNP-based nanozymes for colorimetric detection of serum L-cysteine, *Analyst*, 2023, **148**, 3785–3790, DOI: **10.1039/D3AN00917C**.

63 S. S. M. Ameen, N. M. S. Mohammed and K. M. Omer, Ultra-small highly fluorescent zinc-based metal organic framework nanodots for ratiometric visual sensing of tetracycline based on aggregation induced emission, *Talanta*, 2023, **254**, 124178, DOI: **10.1016/j.talanta.2022.124178**.

64 S. M. Pirot, K. M. Omer, A. H. Alshatteri, G. K. Ali and O. B. A. Shatery, Dual-template molecularly surface imprinted polymer on fluorescent metal–organic frameworks functionalized with carbon dots for ascorbic acid and uric acid detection, *Spectrochim. Acta, Part A*, 2023, **291**, 122340, DOI: **10.1016/j.saa.2023.122340**.

65 B. Han, H. Guan, B. Peng, Y. Zhang and Y. Liu, Fe_3O_4@Au–metal organic framework nanozyme with peroxidase-like activity and its application for colorimetric ascorbic acid detection, *Anal. Methods*, 2022, **14**, 4832–4841, DOI: **10.1039/D2AY01460B**.

66 H. Li, H. Liu, J. Zhang, Y. Cheng, C. Zhang, X. Fei and Y. Xian, Platinum nanoparticle encapsulated metal–organic frameworks for colorimetric measurement and facile removal of mercury(II), *ACS Appl. Mater. Interfaces*, 2017, **9**, 40716–40725, DOI: **10.1021/acsami.7b13695**.

67 L. Zheng, Q. Guo, C. Yang, J. Wang, X. Xu and G. Nie, Electrochemiluminescence and photoelectrochemistry dual-signal immunosensor based on Ru(bpy)32+-functionalized MOF for prostate-specific antigen sensitive detection, *Sens. Actuators, B*, 2023, **379**, 133269, DOI: **10.1016/j.snb.2022.133269**.

68 B. Li, T. Suo, S. Xie, A. Xia, Y. J. Ma, H. Huang, X. Zhang and Q. Hu, Rational design, synthesis, and applications of carbon dots@metal–organic frameworks (CD@MOF) based sensors, *TrAC, Trends Anal. Chem.*, 2021, **135**, 116163.

69 Y. Luo, S. Fan, W. Yu, Z. Wu, D. A. Cullen, C. Liang, J. Shi and C. Su, Fabrication of Au25(SG)18–ZIF-8 Nanocomposites: A Facile Strategy to Position Au25(SG)18 Nanoclusters Inside and Outside ZIF-8, *Adv. Mater.*, 2018, **30**, 1704576, DOI: **10.1002/adma.201704576**.

70 H. Li, Y. Wu, Z. Xu and Y. Wang, In situ anchoring Cu nanoclusters on Cu-MOF: a new strategy for a combination of catalysis and fluorescence toward the detection of H_2O_2 and 2,4-DNP, *Chem. Eng. J.*, 2024, **479**, 147508, DOI: **10.1016/j.cej.2023.147508**.

71 Z. Wang, R. Chen, Y. Xiong, K. Cepe, J. Schneider, R. Zboril, C. S. Lee and A. L. Rogach, Incorporating Copper Nanoclusters into Metal–Organic Frameworks: Confinement-Assisted Emission Enhancement and Application for Trinitrotoluene Detection, *Part. Part. Syst. Charact.*, 2017, **34**(6), 1700029, DOI: **10.1002/ppsc.201700029**.

72 Y. Li, S. Li, M. Bao, L. Zhang, C. Carraro, R. Maboudian, A. Liu, W. Wei, Y. Zhang and S. Liu, Pd nanoclusters confined in ZIF-8 matrixes for fluorescent detection of glucose and cholesterol, *ACS Appl. Nano Mater.*, 2021, **4**, 9132–9142, DOI: **10.1021/acsanm.1c01712**.

73 P. Wei, Z. Ning, S. Ye, L. Sun, F. Yang, K. C. Wong, D. Westerdahl and P. K. K. Louie, Impact Analysis of

Temperature and Humidity Conditions on Electrochemical Sensor Response in Ambient Air Quality Monitoring, *Sensors*, 2018, **18**(2), 59, DOI: **10.3390/s18020059**.

74 R. Jalili, M. Dastborhan, S. Chenaghlou and A. Khataee, Incorporating of gold nanoclusters into metal–organic frameworks for highly sensitive detection of 3-nitrotyrosine as an oxidative stress biomarker, *J. Photochem. Photobiol., A*, 2020, **391**, 112370, DOI: **10.1016/j.jphotochem.2020.112370**.

75 M. Xia, Y. Sui, Y. Guo and Y. Zhang, Aggregation-induced emission enhancement of gold nanoclusters in metal–organic frameworks for highly sensitive fluorescent detection of bilirubin, *Analyst*, 2021, **146**, 904–910, DOI: **10.1039/d0an02076a**.

76 K. Yu, Q. Wang, W. Xiang, Z. Li, Y. He and D. Zhao, Amino-Functionalized Single-Lanthanide Metal–Organic Framework as a Ratiometric Fluorescent Sensor for Quantitative Visual Detection of Fluoride Ions, *Inorg. Chem.*, 2022, **61**, 13627–13636.

77 Y. N. Zeng, H. Q. Zheng, J. F. Gu, G. J. Cao, W. E. Zhuang, J. Di Lin, R. Cao and Z. J. Lin, Dual-Emissive Metal–Organic Framework as a Fluorescent "switch" for Ratiometric Sensing of Hypochlorite and Ascorbic Acid, *Inorg. Chem.*, 2019, **58**, 13360–13369, DOI: **10.1021/acs.inorgchem.9b02251**.

78 Z. Li, G. Liu, C. Fan and S. Pu, Ratiometric fluorescence for sensitive detection of phosphate species based on mixed lanthanide metal organic framework, *Anal. Bioanal. Chem.*, 2021, **413**, 3281–3290, DOI: **10.1007/s00216-021-03264-0**.

79 S. S. Mohammed Ameen, A. Bedair, M. Hamed, F. R. Mansour and K. M. Omer, Repurposing expired metformin to fluorescent carbon quantum dots for ratiometric and color tonality visual detection of tetracycline with greenness evaluation, *Microchem. J.*, 2024, **207**, 111960, DOI: **10.1016/j.microc.2024.111960**.

80 X.-J. Kong, J.-X. Tian, Y.-Z. Fang, T.-L. Chen, R. Yu, J.-Y. He, Z.-Y. Zhang and Q. Xiao, Terbium metal–organic framework/bovine serum albumin capped gold nanoclusters-based dual-emission reverse change ratio fluorescence nanoplatform for fluorimetric and colorimetric sensing of heparin and chondroitin sulfate, *Sens. Actuators, B*, 2022, **356**, 131331, DOI: **10.1016/j.snb.2021.131331**.

81 Q. Li, X. Zhou, L.-L. Tan and L. Shang, MOF-based surface tailoring the near-infrared luminescence property of gold nanoclusters for ratiometric fluorescence sensing of acetylcholinesterase, *Sens. Actuators, B*, 2023, **385**, 133695, DOI: **10.1016/j.snb.2023.133695**.

82 J. Ma, Z. Lu, C. Li, Y. Luo, Y. Shi, P. Alam, J. W. Y. Lam, Z. Wang and B. Z. Tang, Fluorescence ratiometric assay for discriminating GSH and Cys based on the composites of UiO-66-NH2 and Cu nanoclusters, *Biosens. Bioelectron.*, 2022, **215**, 114582, DOI: **10.1016/j.bios.2022.114582**.

83 C. Ma, P. Li, L. Xia, F. Qu, R.-M. Kong and Z.-L. Song, A novel ratiometric fluorescence nanoprobe for sensitive determination of uric acid based on CD@ZIF-CuNC nanocomposites, *Microchim. Acta*, 2021, **188**, 1–10, DOI: **10.1007/s00604-021-04914-x**.

84 X. Hu, X. Liu, X. Zhang, H. Chai and Y. Huang, One-pot synthesis of the CuNCs/ZIF-8 nanocomposites for sensitively detecting H2O2 and screening of oxidase activity, *Biosens. Bioelectron.*, 2018, **105**, 65–70, DOI: **10.1016/j.bios.2018.01.019**.

85 J.-Y. Liu, M.-S. Sheng, Y.-H. Geng, Z.-T. Zhang, T.-T. Wang, L. Fei, J. D. Lacoste, J.-Z. Huo, F. Zhang and B. Ding, In situ encapsulation of oil soluble carbon nanoclusters in ZIF-8 and applied as bifunctional recyclable stable sensing material of nitrofurazone and lysine and fluorescent ink, *J. Mol. Struct.*, 2022, **1269**, 133766, DOI: **10.1016/j.molstruc.2022.133766**.

86 Z. Wang, R. Chen, Y. Xiong, K. Cepe, J. Schneider, R. Zboril, C. Lee and A. L. Rogach, Chemical Sensing: Incorporating Copper Nanoclusters into Metal–Organic Frameworks: Confinement-Assisted Emission Enhancement and Application for Trinitrotoluene Detection (Part. Part. Syst. Charact. 6/2017), *Part. Part. Syst. Charact.*, 2017, **34**, 1700029, DOI: **10.1002/ppsc.201700029**.

87 X. Li, X. Wang, W. Guo, Y. Wang, Q. Hua, F. Tang, F. Luan, C. Tian, X. Zhuang and L. Zhao, Selective detection of alkaline phosphatase activity in environmental water samples by copper nanoclusters doped lanthanide coordination polymer nanocomposites as the ratiometric fluorescent probe, *Biosensors*, 2022, **12**, 372, DOI: **10.3390/bios12060372**.

88 X. Gao, J. Liu, X. Zhuang, C. Tian, F. Luan, H. Liu and Y. Xiong, Incorporating copper nanoclusters into a zeolitic imidazole framework-90 for use as a highly sensitive adenosine triphosphate sensing system to evaluate the freshness of aquatic products, *Sens. Actuators, B*, 2020, **308**, 127720, DOI: **10.1016/j.snb.2020.127720**.

89 Y. Xin, D. Zhang, Y. Zeng, Y. Wang and P. Qi, A dual-emission ratiometric fluorescent sensor based on copper nanoclusters encapsulated in zeolitic imidazolate framework-90 for rapid detection and imaging of adenosine triphosphate, *Anal. Methods*, 2023, **15**, 788–796, DOI: **10.1039/d2ay01932a**.

90 P. Liu, R. Hao, W. Sun, Z. Lin and T. Jing, One-pot synthesis of copper nanocluster/Tb-MOF composites for the ratiometric fluorescence detection of Cu²⁺, *Luminescence*, 2022, **37**, 1793–1799, DOI: **10.1002/bio.4359**.

91 Y. Li, Z. Ren, L. Zhang, N. Bi, J. Gou, L. Jia, J. Wu and J. Xu, Multicolor fluorescent probe based on copper nanoclusters and organometallic frameworks for selective detection of aluminum ions, *Colloids Surf., A*, 2024, **687**, 133542, DOI: **10.1016/j.colsurfa.2024.133542**.

92 X. Hu, J. Tang and Y. Shen, Turn-on fluorescence determination of sulfide based on site-occupying modulation of MOF-copper nanocluster interaction, *Microchim. Acta*, 2022, **189**, 306, DOI: **10.1007/s00604-022-05422-2**.

93 A. Khataee, R. Jalili, M. Dastborhan, A. Karimi and A. Ebadi Fard Azar, Ratiometric visual detection of tetracycline residues in milk by framework-enhanced fluorescence of gold and copper nanoclusters, *Spectrochim. Acta, Part A*, 2020, **242**, 118715, DOI: **10.1016/j.saa.2020.118715**.

94 R. Jalili, M. H. Irani-Nezhad, A. Khataee and S. W. Joo, A ratiometric fluorescent probe based on carbon dots and gold nanocluster encapsulated metal–organic framework for detection of cephalexin residues in milk, *Spectrochim. Acta, Part A*, 2021, **262**, 120089, DOI: **10.1016/j.saa.2021.120089**.

95 Y.-H. Wang, Z.-S. Shao, C. Cheng, J.-L. Wang, Z. Song, W.-J. Song, F. Zheng and H.-S. Wang, Fluorescent oligo-nucleotide indicators for ratiometric microRNA sensing on metal–organic frameworks, *Chem. Eng. J.*, 2022, **437**, 135296, DOI: **10.1016/j.cej.2022.135296**.

96 W. Zhang, X. Jiang, Y. Wu, J. Jiang, X. Liu, Y. Liu, W. Wang, J. Lai and X. Wang, Zeolitic imidazolate framework-8 encapsulating gold nanoclusters and carbon dots for ratio-metric fluorescent detection of adenosine triphosphate and cellular imaging, *Talanta*, 2023, **255**, 124226, DOI: **10.1016/j.talanta.2022.124226**.

97 X. Zhou, X. Wang and L. Shang, Ratiometric fluorescence and visual sensing of ATP based on gold nanocluster-encapsulated metal–organic framework with a smart-phone, *Chin. Chem. Lett.*, 2023, **34**, 108093, DOI: **10.1016/j.cclet.2022.108093**.

98 Y. Nie, X. Tao, H. Zhang, Y. Chai and R. Yuan, Self-assembly of gold nanoclusters into a metal–organic frame-work with efficient electrochemiluminescence and their application for sensitive detection of rutin, *Anal. Chem.*, 2021, **93**, 3445–3451, DOI: **10.1021/acs.analchem.0c04682**.

99 H. Chen, Y. Chang, R. Wei and P. Zhang, Gold nano-clusters encapsulated into zinc–glutamate metal organic frameworks for efficient detection of H_2O_2, *Anal. Methods*, 2022, **14**, 1439–1444, DOI: **10.1039/d2ay00195k**.

100 Q. Tan, R. Zhang, G. Zhang, X. Liu, F. Qu and L. Lu, Embedding carbon dots and gold nanoclusters in metal–organic frameworks for ratiometric fluorescence detection of Cu^{2+}, *Anal. Bioanal. Chem.*, 2020, **412**, 1317–1324, DOI: **10.1007/s00216-019-02353-5**.

101 D. Wei, M. Li, Y. Wang, N. Zhu, X. Hu, B. Zhao, Z. Zhang and D. Yin, Encapsulating gold nanoclusters into metal–organic frameworks to boost luminescence for sensitive detection of copper ions and organophosphorus pesti-cides, *J. Hazard. Mater.*, 2023, **441**, 129890, DOI: **10.1016/j.jhazmat.2022.129890**.

102 Y. Li, X. Hu, X. Zhang, H. Cao and Y. Huang, Unconven-tional application of gold nanoclusters/Zn-MOF composite for fluorescence turn-on sensitive detection of zinc ion, *Anal. Chim. Acta*, 2018, **1024**, 145–152, DOI: **10.1016/j.aca.2018.04.016**.

103 S. Govindaraju, P. Puthiaraj, M.-H. Lee and K. Yun, Photo-luminescent AuNCs@UiO-66 for ultrasensitive detection of mercury in water samples, *ACS Omega*, 2018, **3**, 12052–12059, DOI: **10.1021/acsomega.8b01665**.

104 X.-J. Wu, F. Kong, C.-Q. Zhao and S.-N. Ding, Ratiometric fluorescent nanosensors for ultra-sensitive detection of mercury ions based on AuNCs/MOFs, *Analyst*, 2019, **144**, 2523–2530, DOI: **10.1039/c8an02414f**.

105 X. Bi, L. Li, Q. Niu, X. Liu, L. Luo, H. Jiang and T. You, Highly fluorescent magnetic ATT-AuNCs@ ZIF-8 for all-in-one detection and removal of Hg^{2+}: an ultrasensitive probe to evaluate its removal efficiency, *Inorg. Chem.*, 2023, **62**, 3123–3133, DOI: **10.1021/acs.inorgchem.2c03994**.

106 X. Jiang, H. Jin, Y. Sun, Z. Sun and R. Gui, Assembly of black phosphorus quantum dots-doped MOF and silver nanoclusters as a versatile enzyme-catalyzed biosensor for solution, flexible substrate and latent fingerprint visual detection of baicalin, *Biosens. Bioelectron.*, 2020, **152**, 112012, DOI: **10.1016/j.bios.2020.112012**.

107 F. Su, S. Zhang, H. Ji, H. Zhao, J.-Y. Tian, C.-S. Liu, Z. Zhang, S. Fang, X. Zhu and M. Du, Two-Dimensional Zirconium-Based Metal–Organic Framework Nanosheet Composites Embedded with Au Nanoclusters: A Highly Sensitive Electrochemical Aptasensor toward Detecting Cocaine, *ACS Sens.*, 2017, **2**, 998–1005, DOI: **10.1021/acssensors.7b00268**.

108 T. Qing, K. Zhang, Z. Qing, X. Wang, C. Long, P. Zhang, H. Hu and B. Feng, Recent progress in copper nanocluster-based fluorescent probing: a review, *Microchim. Acta*, 2019, **186**, 670, DOI: **10.1007/s00604-019-3747-4**.

109 Y.-P. Xie, Y.-L. Shen, G.-X. Duan, J. Han, L.-P. Zhang and X. Lu, Silver nanoclusters: synthesis, structures and photo-luminescence, *Mater. Chem. Front.*, 2020, **4**, 2205–2222, DOI: **10.1039/D0QM00117A**.

110 L. Chang, Y. Chen, Z. Meng, Z. Yang, J. Qin, J. Zhou, C. Dai, X. Ji, T. Qin, X. Dou, S. Zhu and G. Zang, Zinc Porphyrin Mixed with Metal Organic Framework Nanocomposites and Silver Nanoclusters for the Electrochemiluminescence Detection of Iodide, *ACS Appl. Nano Mater.*, 2024, **7**, 9031–9040, DOI: **10.1021/acsanm.4c00475**.